



A survey of powertrain configuration studies on hybrid electric vehicles

Weichao Zhuang^a, Shengbo Li (Eben)^{b,*}, Xiaowu Zhang^c, Dongsuk Kum^d, Ziyou Song^e,
Guodong Yin^{a,*}, Fei Ju^f

^a School of Mechanical Engineering, Southeast University, Nanjing 211189, China

^b State Key Lab of Automotive Safety and Energy, Tsinghua University, Beijing 100084, China

^c Department of Mechanical Engineering, University of Michigan, Ann Arbor 48109, USA

^d Graduate School for Green Transportation, KAIST, Daejeon 34051, Republic of Korea

^e Department of Naval Architecture and Marine Engineering, University of Michigan, Ann Arbor 48109, USA

^f School of Mechanical Engineering, Nanjing University of Science and Technology, Nanjing 210094, China

HIGHLIGHTS

- HEV configurations are classified into series, parallel, power-split and multi-mode.
- HEV configuration generation and modeling techniques are introduced.
- Entire design space of HEV configuration is explored exhaustively.
- 14 configuration types of multi-mode HEV are explored and identified.
- Research gaps and future trends of HEV configuration studies are discussed.

ARTICLE INFO

Keywords:

Hybrid electric vehicle
Hybrid powertrain
Configuration
Modeling
Exhaustive search
Multi-mode

ABSTRACT

Global warming, air pollution, and fuel depletion have accelerated the deployment of hybrid electric vehicles (HEVs). Apart from the energy management, the configuration of hybrid powertrains plays a central role in achieving better fuel economy and enhanced drivability. This paper comparatively summarizes the configurations, modeling, and optimization techniques of HEVs. Four types of hybrid powertrain configurations available in the market, i.e., series, parallel, power-split and multi-mode, are introduced firstly, followed by their state-of-the-art and pros/cons. Among all configurations, multi-mode hybrid powertrains are observed to have the potential for utilizing the benefits of the other three types by switching the operating modes. Subsequently, the configuration generation and modeling techniques are summarized. By adopting the automated modeling method, the entire design space can be explored exhaustively, and 14 feasible configuration types are classified based on the binary tree. Finally, the research gaps and future trends of HEV configuration studies are discussed.

1. Introduction

Concerns regarding energy usage and environmental protection have caused governments worldwide to legislate stricter fuel economy and CO₂ emission regulations for ground vehicles. Europe announced the most progressive emissions legislation thus far with an intended target of 95 g of CO₂/km in 2021 [1], and China set a target of 117 g/km by 2020. To meet these regulations, downsized engines, powertrain electrification, lower rolling resistance tire and the use of lightweight materials have been investigated intensively over past decades.

Hybridization is a viable step toward powertrain electrification. The idea of utilizing a hybrid powertrain dates back to 1898, when

Ferdinand Porsche built his first car, the Lohner Electric Chaise, which was powered by both a gasoline engine and an electric motor [2]. The main purpose of the hybrid powertrain in the early stage was to improve the launching performance by using the electric machine to assist the internal combustion engine (ICE). Owing to cost and performance constraints of battery packs, the hybrid design had not been accepted by the retail market until decades later, in the late 1990s.

In 1997, the Toyota Prius was introduced with two power sources: a gasoline engine and a battery pack [3]. This model rapidly became successful owing to its significant fuel-saving benefits. Since then, numerous hybrid vehicles have been launched such as the Honda Insight in 1999 and the Ford Escape Hybrid in 2000. The additional power

* Corresponding authors.

E-mail addresses: lishbo@tsinghua.edu.cn (S. Li (Eben)), ygd@seu.edu.cn (G. Yin).

<https://doi.org/10.1016/j.apenergy.2020.114553>

Received 18 October 2019; Received in revised form 30 December 2019; Accepted 24 January 2020

Available online 15 February 2020

0306-2619/ © 2020 Elsevier Ltd. All rights reserved.

Nomenclature

A^*	characteristic matrix
C_{mode}	Kinematic Relationship Matrix in Bond Graph
D	constraint matrix
$FC_{weighted}$	Mass-weighted Fuel Economy
FC_0	Vehicle Fuel Economy of EPA
F	Internal Force between Gear Teeth of Planetary Gear
H_*	Rows of A^* Matrix and Coupling Vectors
J	Diagonal Matrix
M	Torque Transition Matrix
m	Vehicle Mass
P	Acceleration Transition Matrix
R_*	Rank of H_*
T_*	Torque of Powertrain Device
T	Torque Matrix
V_*	elements of H_{veh}
$\dot{\omega}_*$	Angular Acceleration of Powertrain Device
$\dot{\Omega}$	Angular Acceleration Matrix
$rank(*)$	Rank of Matrix *

Acronyms

AHS	Allison Hybrid System
CD	Charge Depletion
CS	Charge Sustained
DP	Dynamic Programming
DOF	Degree of Freedom

EPA	Environmental Protection Agency
ECMS	Equivalent Consumption Minimization Strategy
ECVT	Electronic Continuously Variable Transmission
CVT	Continuously Variable Transmission
HSD	Hybrid Synergy Drive
THS	Toyota Hybrid System
FUDS	EPA Federal Urban Driving Schedule
GM	General Motor
HEV	Hybrid Electric Vehicle
ISG	Integrated Starter Generator
HWFET	EPA Highway Fuel Economy Driving Schedule
ICE	Internal Combustion Engine
MG	Motor/Generator
NVH	Noise Vibration and Harshness
OEM	Original Equipment Manufacturer
PG	Planetary Gear
PMP	Pontryagin's Minimum Principle
PHEV	Plug-in Hybrid Electric Vehicle
PSD	Power Split Device
EREV	Extended-Range Electric Vehicle
SUV	Sport Utility Vehicle
SOC	State of Charge
RHC	Receding Horizon Optimization
FCV	Fuel-cell electric vehicle
DC	direct current
AC	alternating current

source allows for greater flexibility in engine use while meeting the requirement of driver's demand [4]. Moreover, supernumerary techniques such as regenerative braking and engine shut-down provide alternative methods for achieving better fuel economy and emissions reduction.

To exploit the fuel-saving potential of hybrid electric vehicles (HEVs), appropriate energy management among different power sources is essential because it enables proper power distribution between the engine and the battery. Several studies have reviewed the available energy management strategies and have identified the research gaps in the field [5–8]. The energy management methods can be classified as rule-based and optimization-based strategies [9]. The former is real-time control strategy implemented in production vehicles, which requires time-consuming design and calibration practices [10–12]. Moreover, it is heuristic and cannot guarantee optimality [12,13]. The latter methods are realized by minimizing an infinite- or finite-horizon function of the fuel or battery SOC (state-of-charge) over time. The commonly used optimization-based methods include dynamic programming (DP) [14,15], equivalent consumption minimization strategy (ECMS) [16–18], Pontryagin's minimum principle (PMP) [19,20], and receding horizon optimization (RHC) [21–23]. The main challenge of global optimization methods, i.e., DP, is on the requirement of prior knowledge of driving scenarios, which is often inaccessible in real-time control. Different from DP, ECMS and PMP are local alternatives that can be implemented in real time. Fine tuning of the equivalent fuel consumption factor is usually needed to achieve desirable fuel benefits. In addition, PMP may have convergence problems if the underlying two-point boundary value problem is nonlinear [24,25]. As a finite horizon approximation of global optimization, RHC can repeatedly calculate the optimal action within a predefined prediction horizon to improve real-time powertrain management [26,27]. Recently, reinforcement learning and neural network techniques have become popular in approximately optimal control strategy for varying driving scenarios [28–31]. An interesting study on cruise control for parallel HEVs has been conducted [32] that takes the kinetic energy of

the vehicle body as a third energy storage source and avoids the energy lost in the electro-chemical conversion.

In addition to energy management, the configuration of hybrid powertrain, including the component size and powertrain topology, is also essential for achieving better fuel economy [33–36]. In general, four configuration types are used based on the mechanical connections and power flow among the powertrain components: parallel, series, power-split, and multi-mode. Automobile manufacturers prefer different configuration types because each type has unique strengths and weaknesses. For example, Toyota and Ford introduced the power-split HEVs, which have the best fuel-saving potential, while Germany original equipment manufacturers (OEMs) seem to prefer the parallel HEVs due to the cost consideration [3]. Recently, General Motor (GM) and Honda have focused on developing multi-mode hybrid powertrains because they combine the benefits of other configurations. By changing the coupling mechanism among powertrain components, billions of topologically different designs can be achieved based on quantitative estimation [37].

The numerous available configuration designs make it is difficult for engineers to select the most suitable configuration when developing a new HEV [38]. In the present study, we summarize state-of-the-art of HEV configurations as well as the methods used to generate, model, and optimize the configurations. The contributions of this paper are mainly in twofold:

- (1) HEV configurations available in the market are comprehensively reviewed and are divided into four types according to their characteristics: parallel, series, power-split, and multi-mode. The mechanism and the benefits and limitations of each configuration are comparatively discussed.
- (2) The configuration generation, modeling and optimization techniques are summarized. By using the modeling techniques introduced and brute-force search, all configuration types are explored and are classified according to their functionality and characteristics. Moreover, several useful configuration types other than regular

configuration are introduced. In addition, exploitable research gaps and challenges within the hybrid powertrain research are identified and discussed.

The rest of this paper is organized as follows. Section 2 introduces the HEV types. Section 3 summarizes the general configuration types available in the market. Section 4 introduces the configuration generation and modeling techniques of hybrid powertrains. In Section 5, all possible HEV configuration types are explored by employing brute-force search. Finally, the research gaps in hybrid powertrain designs are discussed in Sections 6 and Conclusions are provided in Section 7.

2. HEV classification by hybridization rate

In general, HEVs can be divided into four types according to the electrification level: micro, mild, and full, HEVs as well as plug-in HEVs (PHEVs) [39]. Table 1 shows their main distinctions.

Micro HEVs usually contain an electric motor often in the form of a small integrated or belted alternator/starter. This electric motor is not involved to drive the vehicle running [40], but is used to shut down the engine at a complete vehicle stop, and then restart when the brake pedal is released. Mild HEVs use a larger electric motor, which enables torque assistance and regenerative braking to achieve better fuel savings [41]. In addition, mild HEVs are typically featured of high voltage electrical systems, e.g., 48 V or 90 V [42,43]. Full HEVs have larger batteries and stronger electric motors than those in micro and mild hybrids, which are often high in cost [9]. They enable the usage of the pure electric (EV) mode for a short duration in city driving. PHEVs essentially have similar characteristics as those of full HEVs but include a larger battery package that can be charged by plugging into the grid [44,45]. This allows PHEVs to be operated in EV mode for extended periods. Two types of PHEVs are available in the market: extended-range electric vehicles (EREVs) and blended PEHVs. The former generally use series configuration, in which the gasoline engine only generates electricity and the electric machine drives the vehicle; an example is the BMW i3 with a range extender. The engine is not fired until the battery is depleted. In the latter, the engine is usually engaged to directly power the vehicle. An electric machine acts as a motor/generator (MG) based on the driving demand and battery SOC level, such as that installed in the Chevrolet Volt.

Fig. 1 shows typical battery SOC ranges and cycling ranges of all four types. The SOC range increases with the hybridization degree. Micro, mild, and full HEVs usually have a narrower SOC window to avoid over-charging or over-discharging.

3. HEV powertrain configuration

The powertrain configurations of HEVs can be divided into four types: parallel, series, power-split and multi-mode.

3.1. Parallel hybrid powertrain

3.1.1. Operation mechanism

In parallel HEVs, both the ICE and MG are connected mechanically with the output shaft (Fig. 2) and can simultaneously provide power to operate the vehicle. The available MG is used to shift the engine operating points to a higher-efficiency area. It acts as a generator at low power demand and as a motor at high power demand. In this way, the engine can work at higher efficiency than that in a conventional vehicle. In addition, parallel hybrids must include a transmission to match high engine speed and low vehicle speed [46].

3.1.2. Sub-types and typical models

The parallel configuration can be considered as an incremental addition to a traditional powertrain and its design requires relatively little investment and engineering effort. Parallel hybrid powertrains can be

further classified into five subtypes according to the location and size of the MG: P₀, P₁, P₂, P₃, and P₄ (Fig. 3) [47].

Subtype P₀ refers to the configuration in which a motor is installed before the ICE and is connected to ICE by a belt. Therefore, it is also known as a belt-driven starter/generator HEV. Owing to the torque limitation of the belt, the starter/generator is always small and can fulfill only the start-stop function [48].

The P₁ subtype refers to the configuration in which the motor is mounted on the crankshaft of the engine. Here, the motor is always referred to as an integrated starter generator (ISG) [49,50]. The installation position of the ISG always restricts its size; this limitation does not allow ISG to provide high torque to operate the vehicle. Only some functions can be fulfilled such as start-stop, regenerative braking and acceleration assistance.

Subtypes P₂ and P₃ are the two most popular variations of parallel HEVs. In these configurations, the motor is mounted on the input and output of the transmission, respectively. The motor in P₂ and P₃ is much larger than that in P₀ and P₁ and has the ability to operate the vehicle at relatively high speeds [46]. Recapturing more regenerative braking and eliminating engine drag result in better energy efficiency than that in other subtypes. Many European and Korean automakers have released P₂-type HEVs such as the Volkswagen Passat hybrid [51] and the Hyundai Sonata Hybrid [52]. In China, BYD used the P₃ subtype in the BYD Qin [53].

The P₄ subtype refers to a parallel hybrid in which the motor is mounted directly on the drive shaft or is incorporated into the hub of a wheel using in-wheel motor technology (Fig. 3 (e)). P₄ is generally not used independently but is combined with other parallel subtypes, P₂ and P₃, particularly in four-wheel drive (4WD) vehicles [54].

Previous studies [55] and [56] have compared the performance of different parallel HEVs. A comparative study through DP was also conducted [57] in which P₂ is shown to have better fuel economy than P₁ owing to its larger motor, and P₂ and P₃ have similar fuel economy benefits.

3.1.3. Limitations and challenges

Parallel HEVs are efficient during city stop-and-go conditions. However, this might not be the most efficient configuration because a mechanical connection still exists between the ICE and the output shaft. In addition, because MG cannot be used to simultaneously charge battery and assist in powering the engine, the power assist and EV operations must be controlled carefully to avoid battery depletion. This problem is exacerbated during city driving, in which frequent start-stops can consume a significant amount of battery energy and force the engine to generate power in its low efficiency area. Because of these drawbacks, parallel HEVs have a smaller market share percentage even a variety of models have become available.

Table 1
Comparison of micro, mild, full and plug-in HEVs [39–44].

Function or component parameters	Types of HEV			
	Micro	Mild	Full	Plug-in
Idle Stop/Start	◆	◆	◆	◆
Electric Torque Assistance		◆	◆	◆
Energy Recuperation		◆	◆	◆
Electric Drive			◆	◆
Battery Charging (during Driving)			◆	◆
Battery Charging (from Grid)				◆
Battery Voltage (V)	12	48–160	200–300	300–400
Electric Machine Power (kW)	2–3	10–15	30–50	60–100
EV Mode Range (km)	0	0	5–10	> 10
CO ₂ Estimated Benefit	5–6%	7–12%	15–20%	> 20%

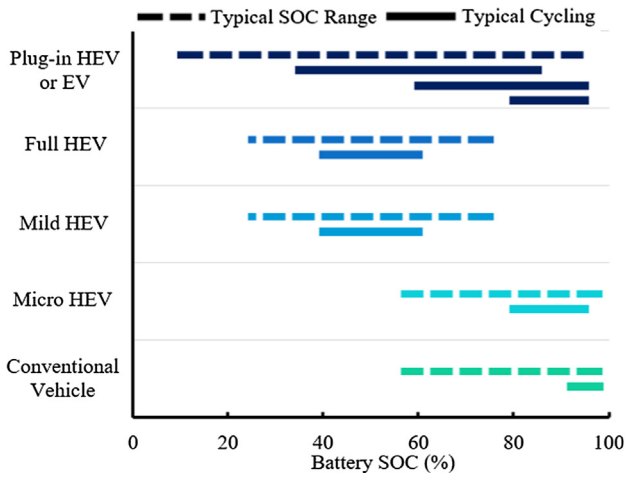


Fig. 1. Typical battery SOC range and typical cycling of micro, mild, full, and plug-in HEVs.

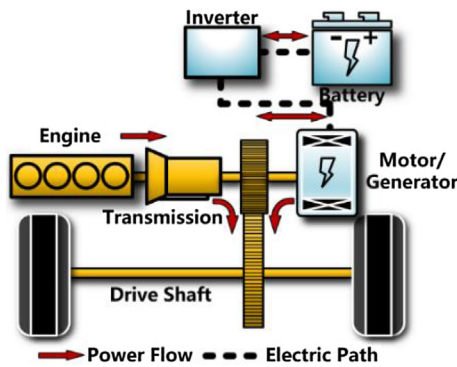


Fig. 2. Configuration of parallel HEV.

3.2. Series hybrid powertrain

3.2.1. Operation mechanism

Series HEVs generally use traction motors to operate the vehicle alone, whereas the ICE is connected to a generator (Fig. 4). The motors are powered by the battery and the generator and can be placed on both front and rear axles to realize electric all-wheel-drive functionality. Since there no mechanical coupling exists between the ICE and vehicle drive axle, the ICE could operate in its best efficiency area regardless of the vehicle speed and power required by the driver. Moreover, the

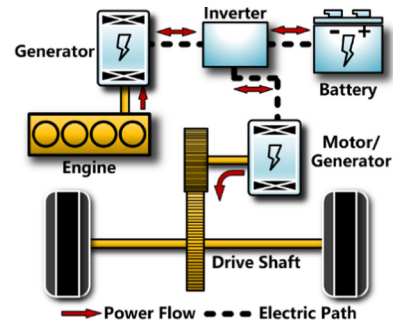


Fig. 4. Configuration of series HEV.

traction motor has a wider operating range and higher efficiency than the ICE. Therefore, a transmission, which is a necessary component in a conventional vehicle, might not be necessary in series HEVs. Thus, the series hybrid powertrain is simpler compared with other types, including configuration and energy management [58].

3.2.2. Typical models

Only a few HEVs in the market use the series configuration expect range-extended HEVs [59]. The most successful model of this type in the market is the BMW i3, which provides an optional gasoline-powered range extender auxiliary power unit [60]. Recently, some OEMs have developed electric cars with range extended technique. A typical example is the Nissan e-Power, which has a 1.2 L gasoline engine that acts solely as a generator for battery charging [61].

3.2.3. Limitations and challenges

The fuel economy of series HEVs can be better than that of conventional vehicles. However, high energy conversion losses can occur because 100% of the engine power must first be converted into electricity. Part of the electricity is stored in the battery, and the remainder powers the motors to propel the vehicle. Even though the MGs have relatively high efficiency and the ICE operates at high efficiency, the multiple energy conversions still result in low overall efficiency. Additionally, the series configuration requires a large traction motor to meet the torque requirement because the motor is the only traction device.

3.3. Power-split hybrid powertrain

3.3.1. Operation mechanism

Power-split HEVs usually employ one or multiple planetary gear (PG) sets to couple the ICE, two MGs and the driveshaft together (Fig. 5)

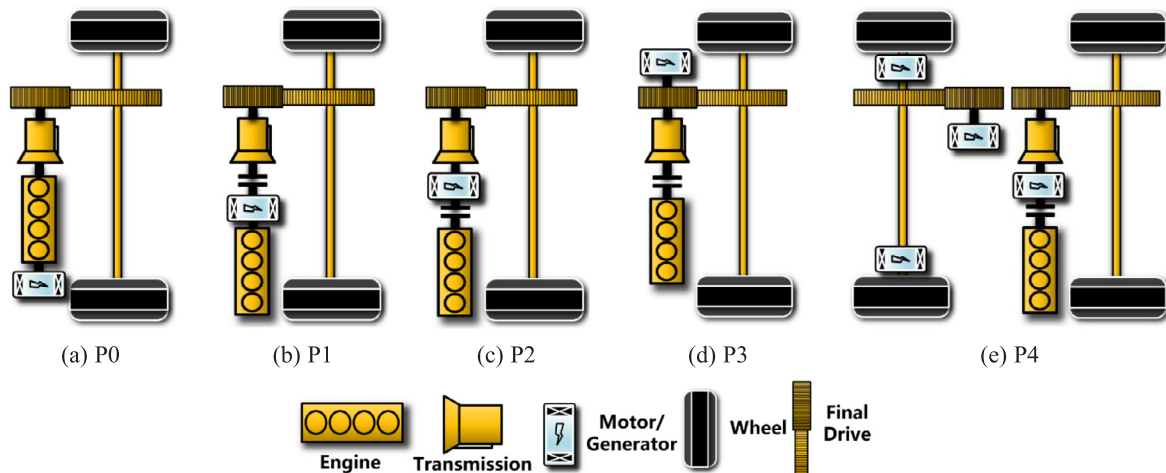


Fig. 3. Configurations of subtypes P_0 to P_4 in parallel HEVs.

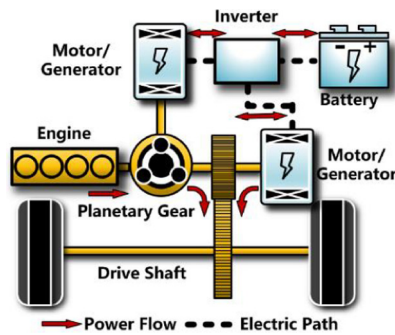


Fig. 5. Configuration of power-split HEV.

[62,63]. The PG sets are the heart of the power-split hybrid powertrain, which is usually referred to as a power split device (PSD). The PSD decouples the ICE from the vehicle speed and acts as a continuously variable transmission (CVT), which results in efficient engine operation regardless of the vehicle speed. Therefore, the PSD in power-split HEVs is also referred to as an electronic-CVT (E-CVT) [64]. Because of this decoupling function, power-split HEVs generally show better fuel economy than both series and parallel HEVs, particularly in city driving conditions.

The PSD allows for power flows from the engine to the driveshaft: either through the mechanical path or the electrical path (Fig. 6) [64,65]. In electrical path, the PSD operates like a series HEV. Part of the ICE power is converted into electricity first by a generator, which drives the motor or charges the battery. In the mechanical path, the PSD also enables the system to operate like a parallel HEV, in which the ICE engine can generate power flow to the driveshaft directly. Therefore, the power-split HEV combines the advantages of both series and parallel hybrids.

3.3.2. Sub-types and typical models

The power-split hybrid powertrain can be further classified into three subtypes according to the point of the power split execution: i.e., input-split, output-split and compound-split [64]. In an input-split HEV, the ICE power is split at the input to the transmission by collocating an MG with the output shaft and sometimes with an additional set of gears in between. In an output-split vehicle, the ICE power is split at the output to the transmission by collocating an MG with the ICE, also sometimes with an additional set of gears in between. In a compound-split vehicle, no MG collocation occurs with the output shaft or the engine.

The most successful power-split hybrid on the market is the input-split subtype, such as the Toyota Hybrid System (THS) or Hybrid Synergy Drive (HSD), introduced by the Toyota Motor Corporation [66]. This subtype was first implemented in the Toyota Prius in Japan in 1997 and was then extended to the company's Camry and Lexus hybrid vehicles in the following years. The second-generation THS was announced in 2004, offering increased system efficiency, enhanced power, and improved scalability [67]. Scalability enables the THS to adapt to different vehicle sizes by changing the reduction paths of ICE/MG1 and MG2. A similar input-split concept was adopted by the Ford Motor Company in its Fusion Hybrid and C-max models. However, General Motor developed two classes of power-split powertrains by using the other two subtypes in a power-split configuration, the Voltex Hybrid Powertrain with an output-split mode [68] and the Allison Hybrid System (AHS) with both an input-split and a compound-split mode [69].

Power-split HEVs have a variety of design variations by changing the locations of the employed components [70]. To explore all possible designs, Liu and Peng proposed an automated modeling method to efficiently build the dynamics of a power-split HEV and identified a design with optimal fuel economy [71]. Bayrak *et al.* enumerated all

feasible powertrain by using a bond graph and generated complete sets of feasible designs based on an exhaustive search [72]. Kim *et al.* re-organized all the possible single PG configurations into a compound-lever design space and screened the optimal design by balancing the fuel benefits and the drivability [73,74].

3.3.3. Limitations and challenges

As discussed in Section 3.3.1, the electrical path incurs higher energy loss than the mechanical path because of the extra energy conversion. More ICE power delivered through the electrical path indicates more energy loss caused by the PSD. When the speed of either MG is equal to zero, the engine-generator-motor path has zero power transmission, and the energy transition is the most efficient. This condition is known as the mechanical point. The energy dissipation in the electrical path might cause power-split HEVs to have greater energy losses than those in parallel HEV in some situations, particularly in high-speed cruising [64].

3.4. Multi-mode hybrid powertrain

3.4.1. Operation mechanism

The multi-mode hybrid powertrain system can be developed by adding clutches to parallel or power-split powertrain systems, which can become any of the three hybrid configurations (series, parallel and power-split) in the same powertrain. Its subtype is also referred to as the operating mode. The freedom to choose from different modes makes it possible to achieve higher energy efficiency and performance than that realized by using the other HEV configuration types introduced above.

3.4.2. Sub-types and typical models

Multi-mode hybrids can be further classified into two subtypes, series-parallel [75] and PG coupling [37], according to whether PG sets are used to couple the powertrain components.

(1) Series-parallel multi-mode configuration

The series-parallel subtype (Fig. 7) was first introduced by Honda in 2014 in its i-MMD system, which is installed in the Accord plug-in hybrid. Two MGs are used in this configuration: One is fully coupled with the ICE, and the other connects directly to the drive shaft [76]. A clutch is employed to disengage the connection between the ICE and output shaft, which enables three operating modes: EV, series, and parallel. The mode shift strategy avoids inefficient engine operation: The EV mode is used when the battery SOC is high, and the series and parallel modes operate only at low and high vehicle speeds. A regular transmission is no longer required to reduce the powertrain cost. Since a mechanical connection still exists between the ICE and the output shaft in the parallel mode, ICE cannot operate in its most efficient area at all vehicle speeds.

(2) PG coupling multi-mode configuration

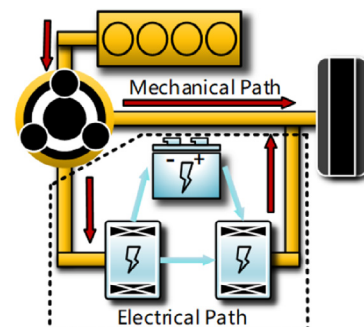


Fig. 6. Power flow of power-split hybrid powertrain.

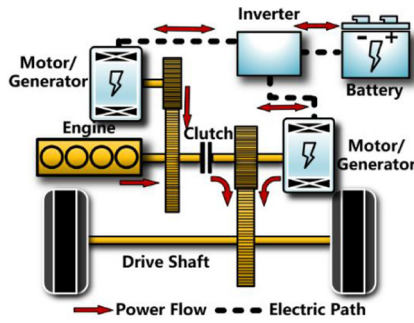


Fig. 7. Configuration of series-parallel hybrid powertrain.

The PG coupling subtype is developed by adding clutches between the PG nodes of in power-split configuration. A typical example is the Advanced Hybrid System patented by General Motors in 2002 (Fig. 8(a)) [69]. By switching the two clutches, two operating modes are achieved: the input-split mode and the compound-split mode. The former mode can provide large output torque, which is more suitable for low speed cruising, whereas the latter tends to have higher efficiency at high speeds by preventing the speed of MG2 from increasing continuously with the vehicle speed. As a result, better fuel economy and launching performance is achieved by proper mode selection, particularly in buses which require higher torque at low speeds.

In addition to AHS, GM in 2011 introduced another multi-mode powertrain known as Voltec which originally had a single PG and three clutches (Gen1) [77], and was later changed to a double-PG design (Gen2) in 2015 (Fig. 8(b)) [68]. The three clutches in the Voltec Gen2 enable five operating modes. Of these modes, Voltec Gen2 has an input-split mode and a compound-split similar to that in AHS, in addition to two EV modes for plug-in functionality.

Toyota developed a multi-mode hybrid powertrain by adding a Ravigneaux-type PG and two clutches to its THS [78,79]. The second MG's gear is switched between high and low ratios for low- and high-speed driving, respectively. To develop a more powerful hybrid system, Toyota combined the THS with a four-speed automatic transmission in 2017 to multiply the output torque (Fig. 8(c)) [80]. This powertrain is the multi-stage hybrid featured in the company's Lexus LC 500 h and LS 500 h models [81].

Although many multi-mode configurations have been proposed and patented, many more remain unexplored [82]. A multi-mode hybrid can be generated in two ways. The first involves changing the locations of the powertrain components, including the engine, two MGs, and the output node to the vehicle drive axle. Each device can connect with any node of the PG sets. In the second method, the number and locations of permanent connection and clutches also result in different hybrid powertrains. Fig. 9 shows all possible clutches and permanent connections of both double and triple PG sets. The total number of possible clutches that connect two nodes, or a node with the ground, is

$$N_{clutch} = C_{3N_p}^2 + 3N_p - 2N_p - 1 \quad (1)$$

where the first term is the number of clutches that can be added between any two nodes, and the second term represents the number of total possible grounding clutches. Since locking any two of the three nodes in a PG produce identical dynamics, the third term eliminates redundant clutches. Finally, the output node should not be grounded.

By changing the locations of the powertrain components and selecting different clutch positions, billions of configurations are available [83]. To explore the enormous design space, smart configuration generation and modeling techniques are required, which will be discussed in Section 4.

3.4.3. Limitations and challenges

The deployment of multiple modes can introduce severe mode shift

problems [84]. Improper mode shifting will increase the noise, vibration, and harshness (NVH) [85]; increase the energy consumption [86]; and reduce the ride comfort [87] and vehicle drivability [88].

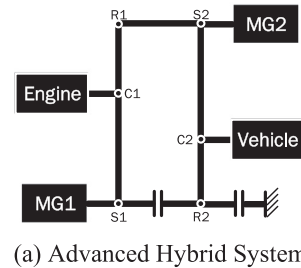
To reduce the negative impacts caused by mode shifts, researchers have begun to investigate mode shifts of series-parallel HEVs, particularly for transitions from EV modes to hybrid-drive modes [89].

In comparison to series-parallel HEVs, PG-based multi-mode HEVs have worse NVH because they rely on PG sets to couple the engine and the driveline mechanically; no any torque converter or clutch is used, which are usually available in series-parallel HEV to passively damp the vibrations and oscillations. Researchers have investigated mode shifts of PG-based multi-mode HEV from two perspectives: mode shift map design [90] and mode transition control. The mode shift duration should be minimized to reduce the torque hole and energy loss during the transition. However, driveline torsional vibrations and torque variation caused by the engine torque pulsations should be suppressed to mitigate the NVH level [85] and improve the vehicle drivability [88,91]. Fortunately, the rapid torque response of electric can compensate for the torque disturbance [92].

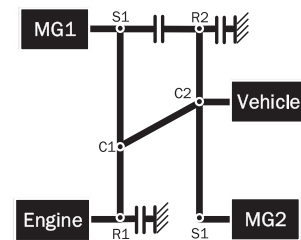
3.5. Short summary

In this subsection, we comparatively study the different configurations by quantitatively summarizing the HEV models available on the market. Table 2 lists the typical productions available and their specifications. The fuel economy is denoted as FC_0 , which is calculated by following the Environmental Protection Agency (EPA)'s practice of 55/45 weights on the city cycle (FUDS) and the highway cycle (HWFET) [93]. For fair comparison, a mass-weighted fuel economy $FC_{weighted}$ is defined in Eq. (2), where m is the vehicle mass.

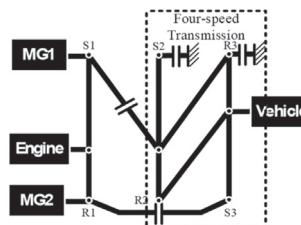
$$FC_{weighted} = \frac{FC_0}{m} \quad (2)$$



(a) Advanced Hybrid System



(b) GM Voltec Gen2 powertrain



(c) Toyota multi-stage hybrid powertrain

Fig. 8. Lever diagram of different multi-mode HEVs.

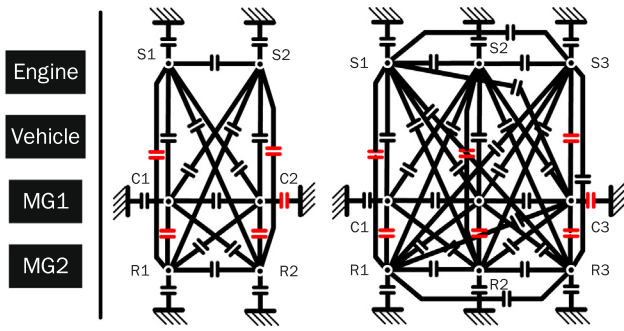


Fig. 9. All possible clutches and permanent connections of both double and triple PG sets.

Fig. 10 shows the comparative results. OEMs apparently prefer different configuration types; most have developed parallel or series-parallel HEVs owing to investment considerations. Toyota and Ford, which own the highest market share, are continually working on the power-split configuration, while GM focuses on the multi-mode for HEV development.

With the improvements in powertrain control techniques, the weighted fuel economy of each vehicle (e.g., Toyota Prius in Fig. 10) is gradually improved with newer models. Currently, the fourth-generation of the Toyota Hybrid Synergy Drive deployed in the Prius 2019 and Camry 2019 claims the best fuel economy among all HEV configurations, no matter in charge-sustained (CS) or charge-depletion (CD) mode [93].

Among all configuration types, power-split and multi-mode HEVs can achieve the best trade-off between fuel economy and drivability. Compared with power-split, the multi-mode type has an even better balance between the fuel economy and acceleration performance because it has the flexibility to adapt to different driving requirements by changing its operating mode. It is predicted that more OEMs will develop the series-parallel or multi-mode hybrid powertrains in the future and that the HEVs will achieve better fuel economy and driving performance with the upgraded powertrain technology.

4. Configuration generation and modeling techniques

As previously discussed, multi-mode hybrids have the best potential for achieving balance between fuel economy and driving performance. However, their designs on the market are relatively limited, and the majority of design space has not yet been considered. To explore such enormous design space, a methodology for generating the configurations and modeling the dynamics is required. Generally, three approaches are discussed in the literature: the graph theoretic method, the bond graph approach and automated modeling.

4.1. Graph theoretic method

Graphs have been used to represent system topologies since the 1700s and are currently adopted in the design of HEV powertrain systems. Silvas [94] proposed an undirected connected finite graph to represent the HEV configuration composed of nodes, or components such as power sources and wheels, and edges, or connections between components such as transmissions and PGs. By defining the functionality and cost constraints, a constraint logic programming problem is formulated. The feasible configurations for all four configuration types can be derived. However, the performance of each generated configuration such as like fuel economy and acceleration performance cannot be evaluated because the proposed undirected graph cannot be used to model the dynamics.

Adam H. Ing [95] used a directed linear graph to represent the powertrain structure. By using the graph theory, a quasi-static model of

the configuration can be generated. The fuel economy and acceleration performance of the designs generated are evaluated based on the equations generated. However, this method cannot be used to model a hybrid powertrain with multiple modes.

4.2. Bond graph

Bond graphs are used to model multi-energy domain systems such as mechanical, electrical, and hydraulic systems and have recently been applied to the modeling of HEV [96,97]. Other than the graph theory, the bond graphs have a notion of causality and allow the modeling of system dynamics.

In bond graphs, power flow is represented by a bond between two nodes and is denoted by a pair of variables known as power variables, i.e., flow and effort, the product of which is the instantaneous power of the bond. For example, in a mechanical system, force is the effort variable, and velocity is the flow variable.

On the basis of the bond graphs, Bayrak [96] proposed a framework to develop single and multi-mode hybrid configurations. By enumerating all undirected graphs for external junctions and internal junctions, assigning 0 and 1-junctions and the bond weights, the design space of the HEV configurations are generated in the form of bond graph representation. A quasi-static model is generated based on the bond graph in the form of state-space representation as shown in Eqs. (3) and (4):

$$\begin{bmatrix} \dot{\omega}_{MG1} \\ \dot{\omega}_{MG2} \end{bmatrix} = -C_{mode} \begin{bmatrix} \omega_{eng} \\ \omega_{out} \end{bmatrix} \quad (3)$$

$$C_{mode}^{-T} \begin{bmatrix} T_{eng} \\ -T_{out} \end{bmatrix} = - \begin{bmatrix} T_{MG1} \\ T_{MG2} \end{bmatrix} \quad (4)$$

where ω_* and T_* are angular acceleration and the corresponding torques of the powertrain devices, respectively, and C_{mode} is the kinematic relationship matrix derived from the bond graphs.

In the Bayrak's framework, the inertia of the engine and MG is ignored which may have a considerable influence on the performance evaluation of HEVs, especially for the mode shift of multi-mode HEVs.

4.3. Automated modeling


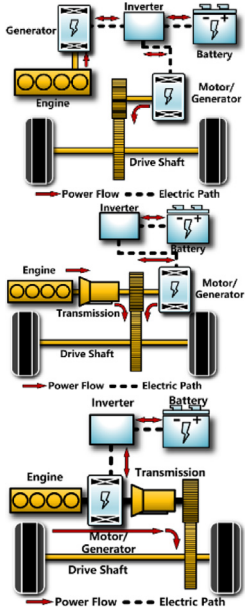











Automated modeling refers to the methodology of modeling the dynamics of the hybrid powertrain automatically by following pre-defined rules. This method was first proposed by Liu and Peng [71] in 2009 for power-split HEVs and was extended to multi-mode HEV modeling by Zhang in 2014 [98]. The core concept of automated modeling is to model the dynamics of the configuration in the state-space representation as follows:

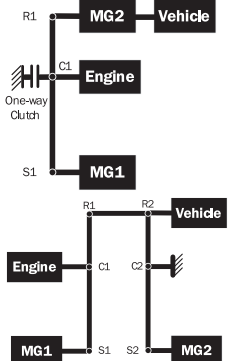
$$\begin{bmatrix} J & D \\ D^T & 0 \end{bmatrix} \begin{bmatrix} \dot{\Omega} \\ F \end{bmatrix} = \begin{bmatrix} T \\ 0 \end{bmatrix} \quad (5)$$

where J is a diagonal matrix with dimensions of $3n \times 3n$, reflecting the inertia on each node, where n is the number of PGs. In addition, D is a $3n \times n$ constraint matrix with entries determined by the connections of PG nodes with the four powertrain components.

For a multi-mode hybrid powertrain consisting of multiple operating modes, each mode has a dynamic model in the form of $A\dot{\Omega} = T$. To accelerate the modeling, Zhang proposed a torque transition matrix M and angular acceleration transition matrix P based on the clutch states [98]. By using the transition matrices, the dynamics of each mode in multi-mode hybrid powertrain are represented by the characteristic matrix A^* as shown in Eq. (6), which governs the relationship between the angular acceleration of powertrain devices ω_* and their corresponding torques T_* .


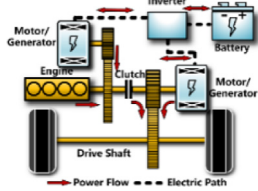


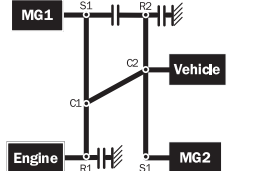


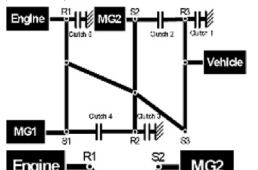

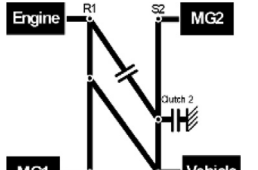

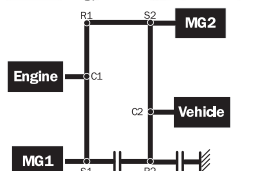

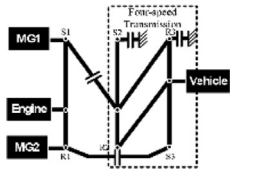
Table 2
Typical HEVs available on the market and their configurations.

Configuration	Automobile company	Model	Photo	Plug-in or not	Fuel economy (MPG or MPGe) [93]	0–60 mph acceleration time	Subtype	Configuration diagram
Series	BMW	i3-ER		Plug-in	35 MPG/111 MPGe	6.5 s	N/A	
	Nissan	Notee-Power		Regular	45 PG	> 10 s	N/A	
Parallel	BYD	Qin		Plug-in	33.2 MPG	5.9 s	P3	
	Volkswagen	Jetta Hybrid		Regular	44 MPG	7.9 s	P2	
	Hyundai	Ioniq Blue		Regular/ Plug-in	52 MPG/119 MPGe	N/A	P2	
		Sonata Hybrid		Regular/ Plug-in	39 MPG/99 MPGe	8.6 s		
	Mercedes-Benz	C350e		Plug-in	30 MPG/51 MPGe	5.9 s	P2	
BWM	Active Hybrid 5		Regular	26 MPG	5.7 s			
Power-Split	Toyota	Prius		Regular/ Plug-in	54 MPG/133 MPGe	9.8 s		
	Ford	Fusion Hybrid		Regular/ Plug-in	42 MPG/103 MPGe	8.5 s		
	Toyota	Camry Hybrid		Regular	52 MPG	7.2 s	Input-Split (Double-PG)	
	Lexus	CT 200 h		Regular	42 MPG	9.8 s		



(continued on next page)

Table 2 (continued)

Configuration	Automobile company	Model	Photo	Plug-in or not	Fuel economy (MPG or MPGe) [93]	0–60 mph acceleration time	Subtype	Configuration diagram
Multi-Mode	Honda	Accord		Regular/ Plug-in	42 MPG/ 110 MPGe	7.6 s	Series-Parallel	
	SAIC Roewe	E550		Plug-in	38.1 MPG	10.5 s		
Chevrolet	Volt		Plug-in	42 MPG/106 MPGe	7.4 s	Double-PG(Five Modes)		
	Malibu Hybrid		Regular	46 MPG	7.4 s			
Cadillac	CT6 Hybrid		Plug-in	25 MPG/ 62 MPGe	5.2 s	Triple-PG(Six Modes)		
Chrysler	Pacifica Hybrid		Plug-in	32 MPG/ 84 MPGe	6.7 s	Double-PG(Three Modes)		
Allison	Advanced Hybrid System (AHS)		Regular	N/A	N/A	Double-PG(Two Modes)		
Lexus	LC 500 h		Regular	30 MPG	5.3 s	Multi-Stage (Ten Modes)		

$$\begin{bmatrix} \dot{\omega}_{out} \\ \dot{\omega}_{eng} \\ \dot{\omega}_{MG1} \\ \dot{\omega}_{MG2} \end{bmatrix} = \begin{bmatrix} a_{11} & a_{12} & a_{13} & a_{14} \\ a_{21} & a_{22} & a_{23} & a_{24} \\ a_{31} & a_{32} & a_{33} & a_{34} \\ a_{41} & a_{42} & a_{43} & a_{44} \end{bmatrix} \begin{bmatrix} T_{load} \\ T_{eng} \\ T_{MG1} \\ T_{MG2} \end{bmatrix} = A^* \begin{bmatrix} T_{load} \\ T_{eng} \\ T_{MG1} \\ T_{MG2} \end{bmatrix} \quad (6)$$

Based on the derived characteristic matrix, the feasibility, functionality and characteristics of each configuration can be determined. Thus, in the following section, we discuss automated modeling to explore all possible configurations of the hybrid powertrain.

5. Configuration exploration and classification

As discussed in Section 3.4, multi-mode hybrid powertrains comprise several sub-configurations with clutches added. These sub-configurations include but are not limited to the configuration types introduced in Section 3: series, parallel, and power-split. In this section, we systematically explore all possible sub-configurations of hybrid powertrains and discuss the characteristics of each configuration.

5.1. Brute-force search and dynamics modeling

As discussed in the literature [37,98], different powertrain component locations may result in different hybrid powertrains. Thus, for simplicity, we fixed these locations to be the same as that in the GM Voltec, as shown in Fig. 11. In this configuration, the ICE connects with the ring gear of the first PG; the vehicle output shaft connects with the carrier gear of the last PG; and the two MGs connect with the sun gears of the first PG and last PG, respectively. In addition, the PG nodes, including the sun, carrier, and ring gears, are numbered in a series in the following description.

Before exploring all possible sub-configurations, the effective number of links that connect PG nodes should be first determined. As the degree of freedom (DoF) of a single PG is two, the DoF of double- and triple-PG hybrid powertrains with no connection begins from four and six, respectively. In this study, the system DoF refers to the number of components with independent speed. Since each effective link reduces the DoF by one, the meaningful DoF of the multi-mode hybrids are 1, 2, and 3 representing the parallel mode, the power-split mode, and the engine speed, respectively, where the speed of one of the MGs is free [83]. Therefore, the effective numbers of links for double- and

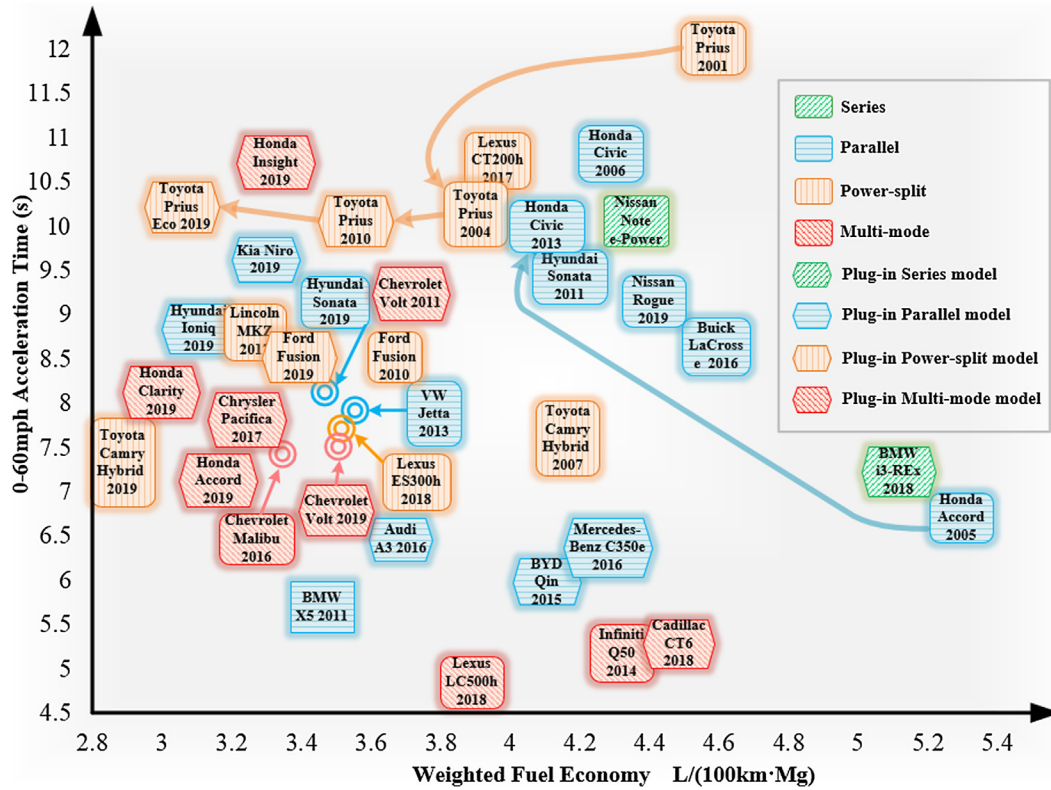


Fig. 10. Typical HEVs available on the market. The weighted fuel economy was calculated by Eq. (2).

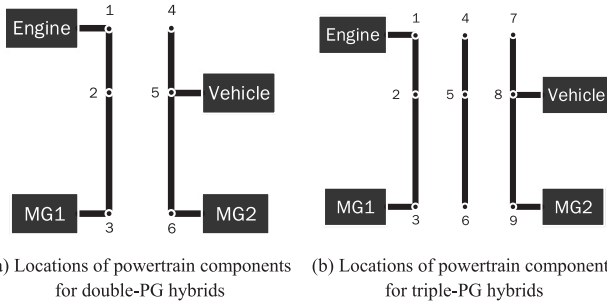


Fig. 11. Locations of powertrain components for double- and triple-PG hybrid powertrains.

triple-PG hybrids are between 1 and 3 and between 3 and 5, respectively. In addition, we assigned to each link a vector composed of the serial numbers of the connected nodes. For example, the link between Node 1 and Node 4 is represented by [1 4]. If Node 1 is grounded, the link is expressed by [1 0], with 0 following the grounded node.

In previous research [37], all possible combination of links inside the double- and triple-PG hybrids are explored exhaustively. It should be noted that any nodes connected by two or multiple links should be first merged. For example, three links in double-PG hybrids, marked as [1 2], [1 4], and [2 4], should be combined and represented by the vector [1 2 4]. In this study, depth-first search was used to traverse all possible connected nodes [99]. Finally, the dynamics of each configuration are represented in the state-space form, as shown in Eq. (6), by the automated modeling methodology introduced in Section 4.3.

5.2. Mode classification

For organizing all sub-configurations, several vectors and coefficients were constructed and extracted from the characteristic matrix A^* . The four rows of the A^* matrix are referred to as H_{veh} , H_{eng} , H_{MG1} , and

H_{MG2} , respectively. The elements of H_{veh} are V_{veh} , V_{eng} , V_{MG1} , and V_{MG2} , which represent the torque contributions of each component to the output shaft. V_{eng} , V_{MG1} and V_{MG2} can be zero if the powertrain components are not connected with the vehicle output.

In addition, six coupling vectors reflecting the coupling relation among powertrain components are defined as $H_{VE} = [H_{veh}; H_{eng}]$, $H_{VMG1} = [H_{veh}; H_{MG1}]$, $H_{VMG2} = [H_{veh}; H_{MG2}]$, $H_{EMG1} = [H_{eng}; H_{MG1}]$, $H_{EMG2} = [H_{eng}; H_{MG2}]$, and $H_{MG1MG2} = [H_{MG1}; H_{MG2}]$. According to the defined vectors, several parameters are listed as follows.

1) Rank of the characteristic matrix A^*

Since each row of A^* in Eq. (6) represents the relationship between the torque input and a component's acceleration, a rank reduction means that the acceleration of one component can be represented as a linear combination of those of the other components. Herein, the number of accelerations that can be represented by other components is determined by the number of the independent accelerations, which represents the DoF defined at the beginning of this section. However, the rank of the characteristic matrix, $rank(A^*)$, is the dimension of the torque input or the component's acceleration on the basis of linear algebra, which also refers to the number of linearly independent accelerations. Therefore, the DoF of the system equals the rank of its characteristic matrix, $rank(A^*)$:

$$DoF = rank(A^*) \quad (11)$$

2) Rank of the coupling matrix H_{VE} , H_{VMG1} , H_{VMG2} , H_{EMG1} , H_{EMG2} and H_{MG1MG2}

Similar to the rank of the characteristic matrix A^* , the rank of the coupling matrix can represent the correlation between the two components in that matrix. For example, if the rank of H_{VE} is equal to 1, the acceleration of the vehicle is proportional to the acceleration of the engine. This means that the vehicle output shaft is coupled with the engine directly. On the contrary, a rank of H_{VE} equal to 2 means that the acceleration of the vehicle and the engine are independent of each other. In the following section, the ranks of the matrices H_{VE} , H_{VMG1} , H_{VMG2} , H_{EMG1} , H_{EMG2} , and H_{MG1MG2} refer to R_{VE} , R_{VMG1} , R_{VMG2} , R_{EMG1} ,

R_{EMG2} and R_{MG1MG2} , respectively.

In this section, all configurations explored in Section 3.1 are classified by layers based on the parameters defined by the binary tree, as shown in Fig. 12. To summarize, all 14 valid configuration types and their classification criteria are listed in Table 3. In addition, the numbers of all configuration types are summarized. The unique configuration in Table 3 refers to sub-configurations that share the same characteristic matrix even with different topologies. Fig. 13 shows an example of multiple topologies having different links but the same dynamics because Nodes C1, R2, C2, S2, and C3 all have the same rotational speed. In this study, configurations sharing the same dynamics are considered to be equivalent; thus, only one is extracted as a unique configuration.

Table 3 lists the number of feasible configurations and unique configurations for both double- and triple-PG hybrid powertrains determined after screening the infeasible and redundant configurations. The triple-PG powertrains have almost 100 times the number of feasible configurations than those of double-PG powertrains originally. After the equivalent configuration screening, only 102 and 4,041 unique configurations were retained. Performance analysis of all unique configurations has been conducted in previous research [100].

5.3. Discussion on each sub-configuration

In this section, all 14 sub-configuration types derived above are discussed separately, and examples of a double-PG system are used to demonstrate their functionality and characteristics.

5.3.1. Series configuration

According to the series configuration introduced in Section 3.2, the DoF of the series mode is two. Fig. 14 shows two examples, in which one MG is coupled with the engine mechanically through the first PG set, and the other MG drives the vehicle by grounding the R2 node. Since the engine is not mechanically connected with the wheels, the engine corresponding coefficient V_{eng} in the H_{veh} is zero. In addition, two MGs are mechanically connected with the engine and wheels separately, leading to $V_{MG1}V_{MG2} = 0$, $V_{MG1}^2 + V_{MG2}^2 \neq 0$, and $H_{eng}(3)^2 + H_{eng}(4)^2 \neq 0$.

5.3.2. 3 DoF configuration

The 3 DoF configuration, as shown in Fig. 15(a), means that three controllable independent speeds are available in the hybrid powertrain. Therefore, the speeds of the vehicle and engine as well as the speed of one of the two MGs can be controlled independently. That is, three linearly independent equations are required to describe the speed relationship among the powertrain components. Since the number of controllable powertrain components and the DoF are both three, there is no flexibility in the component torque selection when their accelerations are determined. This can also be observed from Eq. (6): assuming the first three rows of the A^* matrix are used to calculate the torque commands, the torques from all three powertrain components are determined on the basis of the desired component acceleration because the resistance torque T_{load} is not a control variable. This phenomenon may lead to inefficient system operation. Moreover, the component speed will become uncontrollable when the engine is off. Therefore, the 3 DoF configuration is not suitable for topologies with a single output shaft [101].

By adding an extra output shaft, as shown in Fig. 15(b), the 3 DoF system will become effective. By connecting the two output shafts with the front-rear or left-right wheels, 4WD [102] or the differential steering function [103] can be achieved.

5.3.3. Compound, input and output-split configuration

As introduced in Section 3.3, the input-split, output-split, and compound-split configurations all belong to the power-split configuration and are collectively known as ECVT modes. All of these ECVT modes have two DoFs, which enables decoupling of the engine speed from the vehicle speed.

The differences between them are the coupling relationship among the vehicle, engine and two MGs [64]. In the input-split configuration, the speed of one MG is coupled with the vehicle speed, whereas the speeds of the engine and the other MGs are uncoupled with the vehicle speed, as shown in Fig. 16 (i.e., $R_{VMG1}R_{VMG2} = 2$). On the contrary, the engine speed of the output-split configuration is always coupled with one MG and is uncoupled with the speeds of the other MG and the vehicle, as shown in Fig. 17 (i.e., $R_{EMG1}R_{EMG2} = 2$). If the speeds of the vehicle, engine, and the two MGs are not coupled with each other, as depicted in Fig. 18 (i.e., $R_{EMG1}R_{EMG2} = 4$, $R_{VMG1}R_{VMG2} = 4$, $R_{VE} = 2$, $R_{MG1MG2} = 2$), the compound-split configuration is implied. The

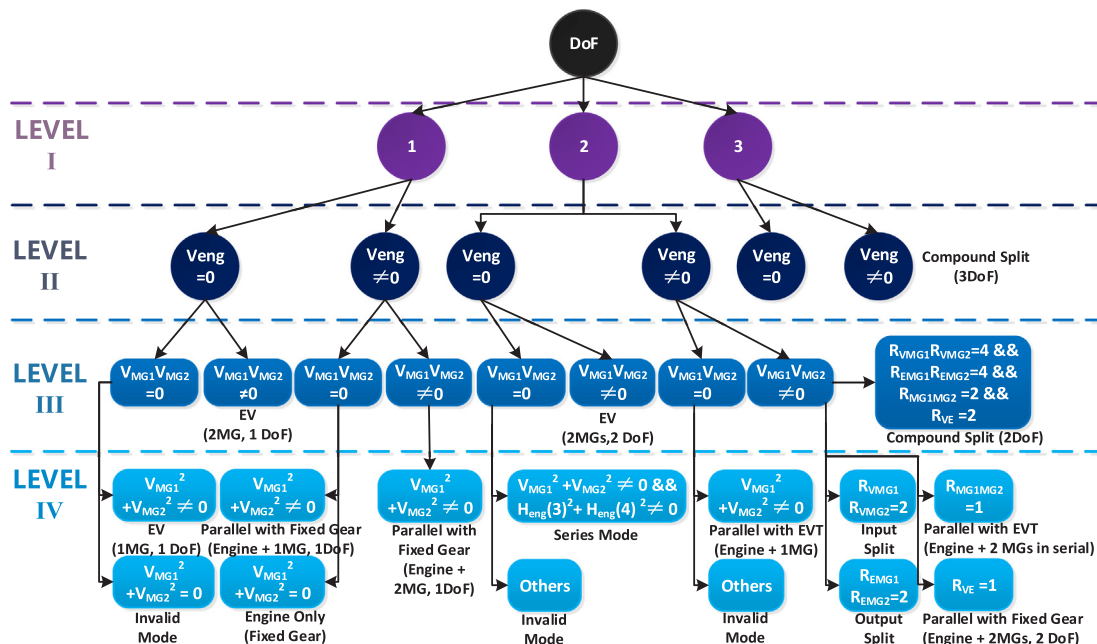


Fig. 12. Configuration classification by binary tree.

Table 3
Classification criteria and number of feasible configurations for 14 configuration types.

Configuration type	Classification criteria	Number of feasible configurations		Number of unique configurations	
		Double PG	Triple PG	Double PG	Triple PG
1 Series configuration	$DoF = 2, V_{eng} = 0, V_{MG1}V_{MG2} = 0, H_{eng}(3)H_{eng}(4) = 0, V_{MG1}^2 + V_{MG2}^2 \neq 0, H_{eng}(3)^2 + H_{eng}(4)^2 \neq 0$	9	70,978	5	85
2 Compound split (3 DoF)	$DoF = 3$	2	88,30	2	650
3 Compound split (2 DoF)	$DoF = 2, V_{eng} \neq 0, V_{MG1}V_{MG2} \neq 0, R_{VE} = 2, R_{VMG1}R_{VMG2} = 4, R_{EMG1}R_{EMG2} = 4, R_{MG1MG2} = 2$	4	2,175	4	269
4 Input split	$DoF = 2, V_{eng} \neq 0, V_{MG1}V_{MG2} \neq 0, R_{VMG1}R_{VMG2} = 2$	13	12,390	6	172
5 Output split	$DoF = 2, V_{eng} \neq 0, V_{MG1}V_{MG2} \neq 0, R_{EMG1}R_{EMG2} = 2$	13	13,227	6	210
6 ECVT with one MG	$DoF = 2, V_{eng} \neq 0, V_{MG1}V_{MG2} = 0, V_{MG1}^2 + V_{MG2}^2 \neq 0$	4	2,394	4	106
7 ECVT with two MGs in series	$DoF = 2, V_{eng} \neq 0, V_{MG1}V_{MG2} \neq 0, R_{MG1MG2} = 1$	3	2,388	3	82
8 Engine only	$DoF = 1, V_{eng} \neq 0, V_{MG1}V_{MG2} = 0, V_{MG1}^2 + V_{MG2}^2 = 0$	17	10,594	4	47
9 Parallel with fixed gear (2 MGs, 2 DoF)	$DoF = 2, V_{eng} \neq 0, R_{VE} = 1, V_{MG1}V_{MG2} \neq 0$	3	1,833	3	82
10 Parallel with fixed gear (2 MGs, 1 DoF)	$DoF = 1, V_{eng} \neq 0, V_{MG1}V_{MG2} \neq 0$	330	240,530	21	1,218
11 Parallel with fixed gear (1 MG, 1 DoF)	$DoF = 1, V_{eng} \neq 0, V_{MG1}V_{MG2} = 0, V_{MG1}^2 + V_{MG2}^2 \neq 0$	80	68,376	24	666
12 EV (2 MGs, 2 DoF)	$DoF = 2, V_{eng} = 0, V_{MG1}V_{MG2} \neq 0$	2	1,279	2	55
13 EV (2 MGs, 1 DoF)	$DoF = 1, V_{eng} = 0, V_{MG1}V_{MG2} \neq 0$	40	35,049	12	331
14 EV (1 MG, 1 DoF)	$DoF = 1, V_{eng} = 0, V_{MG1}V_{MG2} = 0, V_{MG1}^2 + V_{MG2}^2 \neq 0$	76	83,527	6	68
	Sum	596	553,570	102	4,041

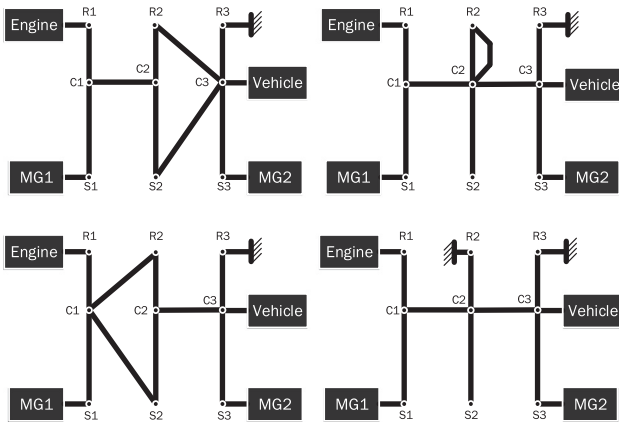


Fig. 13. Example of topologies sharing the same dynamics [100].

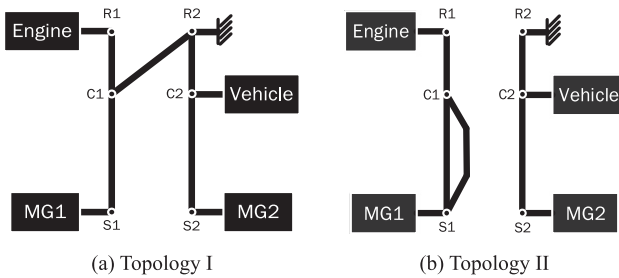


Fig. 14. Examples of series configuration.

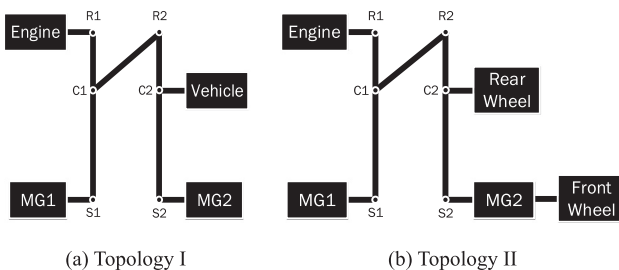


Fig. 15. Examples of 3 DoF configuration.

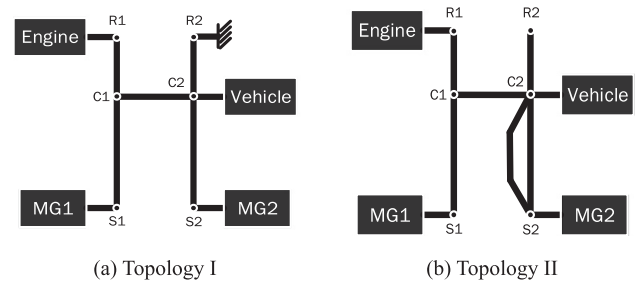


Fig. 16. Examples of input-split configuration.

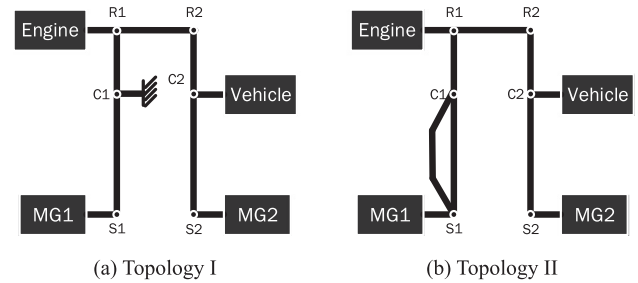


Fig. 17. Examples of output-split configuration.

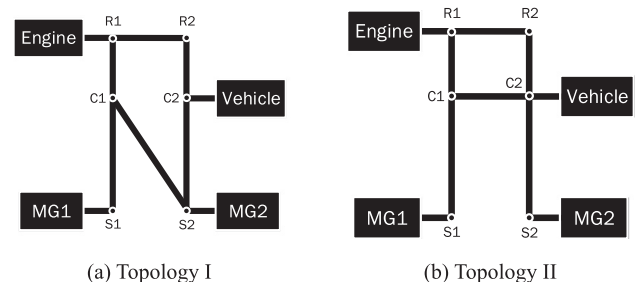


Fig. 18. Examples of compound-split configuration.

structural feature described above results in different positions of the power split for different ECVT types, as mentioned in Section 3.3.

In addition to these structural differences, one of the MGs in an input-split configuration that has a fixed gear ratio with the vehicle

output shaft can provide significant torque assist when launching the vehicle. This attribute makes this configuration type more effective than the other two types under low speeds and can still be feasible in high speeds if the motor maximum speed allows. This configuration is widely applied in Toyota hybrid vehicle fleets [66]. In comparison with the input-split configuration, the compound-split configuration can provide flatter output torque and has a wider speed range. In addition, the existence of two mechanical points makes the compound-split more efficient under some working conditions, such as that at high speeds. Therefore, it is employed in some multi-mode HEVs such as the Chevrolet Volt Gen2 as a high-speed mode [68] to improve the overall vehicle fuel economy. Nevertheless, the output-split configuration has no extraordinary features and is therefore rarely used vehicle production.

5.3.4. ECVT with one motor/two MGs in serial configuration

An ECVT with one motor can be viewed as a one-motor case of input-split configuration without MG coupling with the vehicle output shaft, as shown in Fig. 19 (a) (i.e., $\text{DoF} = 2$, $V_{\text{eng}} \neq 0$, $V_{\text{MG1}}V_{\text{MG2}} = 0$, and $V_{\text{MG1}}^2 + V_{\text{MG2}}^2 \neq 0$). However, an ECVT with two MGs in a series is similar to that shown in Fig. 19 (b), although the two MGs are connected in a series and can be considered as one larger MG (i.e., $R_{\text{MG1MG2}} = 1$).

In this configuration type, the vehicle is still propelled simultaneously by the engine and one MG through the PG set. Such a powertrain arrangement provides an ECVT function with the help of the MG so that the engine speed can be controlled regardless of the vehicle speed. However, it does not offer the same flexibility in controlling the engine torque. The DoF of this powertrain is two, but only two controllable powertrain components are retained, i.e., the engine and one MG. Thus, similar to that in the 3 DoF configuration, the DoF of the torque input is only one, so that the engine torque cannot be arbitrary assigned when the engine is operating at the desired speed.

Even considering these limitations, some researchers proposed powertrains including this configuration type because of its ECVT function. Yang [47] and Zhu [82] both developed power-split hybrid powertrains with a single MG. The uncontrollable engine torque makes such a configuration type limited while the vehicle is operated. As a result, although it is rarely applied in the vehicles produced, it can be used as an intermediate mode in some multi-mode hybrid powertrains when mode shift occurs and the component speeds need to be changed for clutch engagement conditions [104].

5.3.5. Engine-only configuration

In the engine-only configuration, both MGs cannot provide power to operate the vehicle, as shown in Fig. 20. In this circumstance, the output shaft is driven only by the engine with a fixed-gear ratio, which is the same as that in a conventional vehicle without MGs. Therefore, the advantages of powertrain hybridization disappear, which makes this configuration less desirable in multi-mode hybrid powertrains.

5.3.6. Parallel with fixed-gear configuration (2 MGs, 2 DoFs)

The engine in this configuration type is connected to the drive shaft mechanically with a fixed gear ratio (i.e., $V_{\text{eng}} \neq 0$, $R_{\text{VE}} = 1$), whereas the speeds of the two MGs are both decoupled from the vehicle speed through the PG set (i.e., $\text{DoF} = 2$, $V_{\text{MG1}}V_{\text{MG2}} \neq 0$), as shown in Fig. 21.

This topology is recognized as a parallel configuration because the engine speed is coupled to the vehicle speed, which is the same as that in parallel HEVs. With the help of MGs, the torque of the engine can be regulated to achieve higher engine efficiency.

In this configuration type, since the speed of the MGs can be manipulated, higher efficiency could be achieved compared with the configuration type in which the MG speed is proportional to the vehicle speed. However, this configuration was found to be topologically feasible only through the exhaustive search; to the best of our knowledge, it has not been adopted in any commercialized vehicles.

5.3.7. Parallel with fixed-gear configuration (1 MG/2 MGs, 1 DoF)

The parallel with fixed-gear configuration is the exact parallel configuration introduced in Section 3.1, in which the engine and MGs speeds are all proportional to the vehicle speed. If one of the MGs is grounded, the topology is parallel with fixed-gear configuration (1 MG, 1 DoF), as shown in Fig. 22. Otherwise, the topology is marked as parallel with fixed-gear configuration (2 MGs, 1 DoF), and both MGs can either assist or recuperate energy from the vehicle, as shown in Fig. 23.

Different gear ratios between the engine and the output shaft will result in different parallel modes. The triple-PG powertrain can achieve a higher gear ratio (up to 14) if the ring/sun gear ratios are determined [37]. The higher gear ratios are beneficial for buses, sport utility vehicles (SUVs), and trucks, which require high traction torque for acceleration, climbing and towing [83]. In addition, if the gear ratio is appropriate, the parallel configuration may have better efficiency than the ECVT modes at high vehicle speeds because less energy loss occurs in the electrical path, as discussed in Section 3.3.

In addition, the parallel with fixed-gear configuration has the maximum configuration numbers among all 14 configuration types, as shown in Table 3. Naturally, this configuration is easily combined with other configuration types to form a multi-mode hybrid powertrain.

5.3.8. EV (2 MGs, 2 DoFs)

For one of the EV modes, the speeds of both MGs are decoupled from the vehicle speed, which is referred to as EV (2 MGs, 2 DoFs). In addition, the engine is always disabled or grounded, as shown in Fig. 24. Compared with conventional EV mode, in which the MGs are connected with the driveshaft directly, this 2 DoF EV can tune the speeds of both MGs to potentially achieve higher operation efficiency. Zhang proposed a dual-motor-driven electric bus adopting this configuration type that achieved excellent energy efficiency [105].

5.3.9. EV (1 MG/2 MGs, 1 DoF)

For EV modes with 1 DoF, the engine is disabled or grounded by a grounding clutch, and the MGs are connected with the output shaft mechanically with fixed gear ratios as shown in Fig. 25 in the 2 MG case in and Fig. 26 in the 1 MG case. Unlike that in the EV mode with 2 DoFs, the MGs' speeds are coupled with the vehicle speed.

For the EV mode with two MGs, the torques of the MGs can be superimposed to achieve improved launching performance without running the engine. Moreover, instead of tuning the MG speed in EV mode with 2 DoFs, the torques of both MGs can be manipulated to achieve better efficiency while satisfying the driver's demand.

6. Research gaps and future trends

As reviewed so far, great efforts have been made in the field of HEV configuration optimization. However, developing an economic hybrid powertrain with superior performance remains a challenge. In addition, the emergence of vehicle automation, connectivity, artificial intelligence, and fuel cell technology has provided a great opportunity to

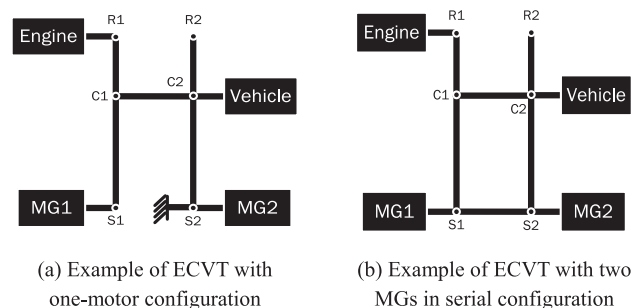


Fig. 19. Examples of ECVTs with one motor/two MGs in serial configuration.

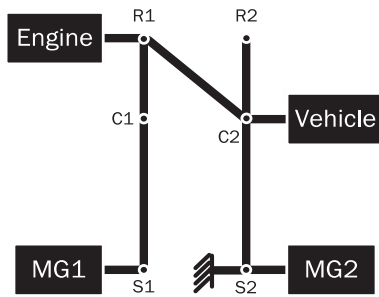


Fig. 20. Example of engine-only mode.

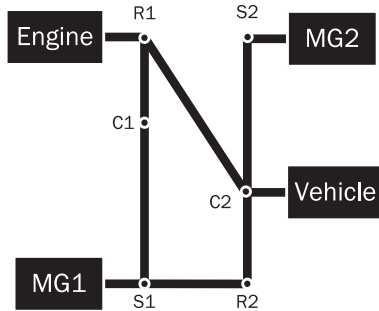


Fig. 21. Example of parallel with fixed-gear mode (2 MGs, 2 DoFs).

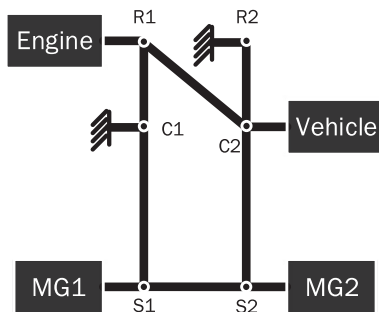


Fig. 22. Example of parallel with fixed-gear configuration (2 MGs, 1 DoF).

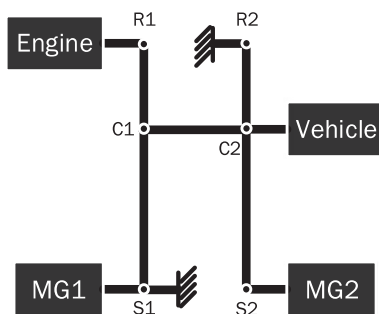


Fig. 23. Example of parallel with fixed-gear configuration (1MG, 1 DoF).

further improve the fuel economy, driving performance and mobility. The research gaps and future trends are discussed in the following subsections.

6.1. Multi-objective configuration optimization

In addition to realizing fuel economy, challenges such as the capital cost [106], generated emissions [107], drivability, performance, and ride comfort turns an optimal design of a hybrid powertrain into a nonlinear multi-objective constrained optimization problem. For a multi-mode hybrid powertrain, drivability and ride comfort during the

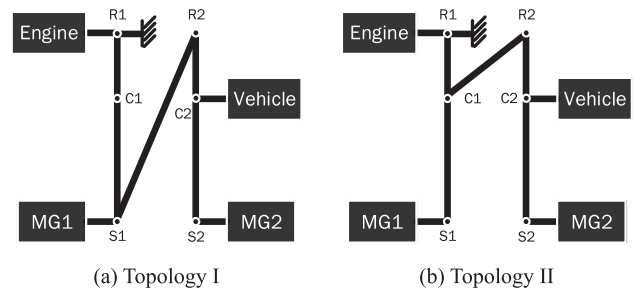


Fig. 24. Example of EV (2 MGs, 2 DoFs).

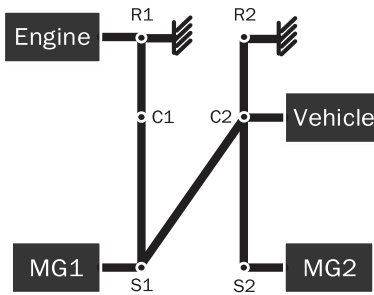


Fig. 25. Example of EV (2 MGs, 1 DoF).

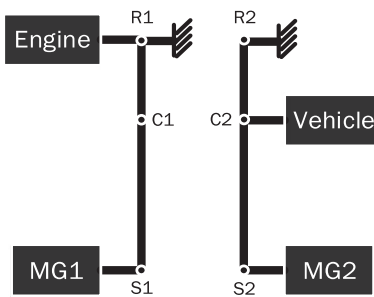


Fig. 26. Example of EV (1 MG, 1 DoF).

mode transition are particularly important in delivering this concept to the market [104]. In addition, the impact of transmission efficiency with a more complicated powertrain configuration has not been studied systematically thus far. Furthermore, owing to the critical fuel economy standards, hybrid technology must be extended to light trucks and SUVs in the near future. Accordingly, 4WD operation is an important feature for both light trucks and SUVs to meet the requirements of heavy acceleration, towing, and climbing. Therefore, the configurations with 4WD that maintain the ECVT function require further investigation [103].

6.2. Integrated optimization in HEV system-level design

To meet more stringent fuel economy and emission regulations, OEMs and researchers have investigated more complex hybrid configurations with multiple planetary gear sets and clutches. Therefore, integration of the concurrent plant design (i.e., configurations and component sizes) with control optimization is needed, which would create unprecedented complexity in the optimization, as shown in Fig. 27 [7]. Since current methods have failed to explore the entire design space exhaustively owing to the computational burden, optimizing the physical parameters and the controls of HEV efficiently remain a challenge.

6.3. Expansion of optimization to connected and automated HEVs

Current HEV configuration optimization and energy management

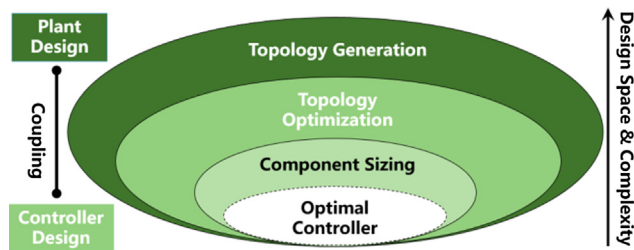


Fig. 27. Plant and control optimization of HEVs.

studies generally focus on a few standard driving cycles such as highway, in-city, and inter-urban for evaluating fuel economy. However, standard fuel economy testing for regulatory purposes does not adequately consider real-world (or off-cycle) driving behavior. Therefore, a variety of research have been conducted to achieve ecological driving (eco-driving) in real-world driving conditions, including highways with altitude variations [108] and city driving with traffic signals [109].

Developments in vehicle connectivity and automation provide additional opportunities for energy efficiency improvements in real-world driving. For example, connectivity can allow a vehicle to predict its future driving conditions with respect to the anticipated road state considering slopes and speed limits as well as the timing of traffic signal phases and car following [110]. The look-ahead or preview information can be used for co-optimization of vehicle dynamics and powertrain (VD & PT) control to maximum the energy efficiency over a portion of a trip or an entire trip [111]. Thus, it is interesting to implement the co-optimization of VD & PT control on a single-vehicle basis, across co-operating vehicles, or even in entire vehicle fleet, to enhance the overall energy efficiency and safety. In addition, integration of VD & PT control technologies with configuration optimization can be promising feature in vehicle designs for a certain application.

6.4. Optimization of fuel cell electric vehicles

Fuel-cell electric vehicles (FCVs) have received significant attention owing to their zero emission of greenhouse gases. These vehicles usually adopt fuel cells as the primary power source, and an additional energy storage system (e.g., batteries or ultra-capacity) is used as an auxiliary power source. Thus, these vehicles are sometimes referred to as fuel cell hybrid electric vehicles. Since fuel cell system have much higher energy density compared to battery system, this type is more promising for heavy duty applications.

The configuration and energy management strategy design of FCVs need to be carefully considered to ensure efficient and smooth operation of the vehicles [112]. Since energy management strategies have been investigated widely, the topology and size of the auxiliary power source (e.g., batteries, ultra-capacity or their combination) [113] and converters (e.g., direct current (DC)/DC and DC/alternating current (AC)) [114] should be optimized further to improve the lives of both the fuel cells and the batteries. Moreover, the interactions between control strategy and configurations should be investigated further to explore the potential of hybridization [7]. The co-optimization, taking their coupling into account, may be the promising method to identify better designs [115,116].

In addition, researchers have recently used multiple fuel cell stacks to simultaneously improve the fuel economy and the durability of the onboard fuel cells [117]. However, techniques for globally optimizing the number of fuel cell stacks and the capacity of the fuel cell stack and the auxiliary power source are essential for enhancing the overall efficiency and cost effectiveness of the vehicle.

6.5. Charging infrastructure

Developing the charging infrastructures is crucial for promoting the EV or PHEV to achieve the sustainable mobility [118,119]. There are some open charging-related problems and challenges to be addressed from the technical and scientific point of view, including the design and optimization of AC charging devices, DC fast charging technology and wireless charging [120]. In addition, Vehicle to Grid (V2G) technology is recognized as a promising technology to integrate the stationary energy storage systems and renewable energy sources with the main grid [121].

7. Conclusions

This study focuses on the survey of the configurations, modelling and optimization techniques of hybrid powertrain. First, four configurations—series, parallel, power-split, and multi-mode—are categorized according to mechanical connections and power flow among the powertrain components. The operation mechanism, state-of-the-art and pros/cons of each configuration comparatively are compared. The multi-mode hybrid powertrain showed the best fuel savings potential because it utilizes the benefits of the other three types. The complexity of multi-mode hybrid powertrain results in a large design space. Second, the configuration generation methods are summarized, including graph theoretic method, bond graph and automated modeling. By using the automated modeling, the design space of HEV configurations was explored exhaustively, and 14 feasible configuration types were classified by using a binary tree. In addition, the features and pros/cons of each sub-configuration are discussed. Finally, the research gaps and future trends on the study of HEV configurations were discussed. To identify a market competitive HEV product, solving the HEV design problem in the system level is expected, which could achieve the co-optimization of plant and control strategy. In addition, there remains a challenge to extend the regular HEV to a connected, automated or fuel-cell powered vehicle.

Declaration of Competing Interest

The authors declare that they have no known competing financial interests or personal relationships that could have appeared to influence the work reported in this paper.

Acknowledgement

This work was supported by National Science Foundation China (No. 51805081, U1664258, 51575103) and National Key R&D Program in China with grant (No. 2016YFB0100906, 2016YFD0700905).

References

- [1] Yang Z, Bandivadekar A. 2017 Global update: light-duty vehicle greenhouse gas and fuel economy standards. https://www.theicct.org/sites/default/files/publications/2017-Global-LDV-Standards-Update_ICCT-Report_23062017_vf.pdf; 2017 [accessed 19.04.29].
- [2] Wakefield EH. History of the electric automobile-hybrid electric vehicles. Society of Automotive Engineers 1998.
- [3] Duoba M, Ng H, Larsen R. Characterization and comparison of two hybrid electric vehicles (HEVs)-Honda Insight and Toyota Prius. *Appl Phys Lett* 2011;99(25):2463.
- [4] Chan CC. The state of the art of electric, hybrid, and fuel cell vehicles. *P IEEE* 2007;95(4):704–18.
- [5] Sabri MFM, Danapalasingam KA, Rahmat MF. A review on hybrid electric vehicles architecture and energy management strategies. *Renew Sust Energ Rev* 2016;53:1433–42.
- [6] Enang W, Bannister C. Modelling and control of hybrid electric vehicles (A comprehensive review). *Renew Sust Energ Rev* 2017;74:1210–39.
- [7] Silvas E, Hofman T, Murgovski N, et al. Review of optimization strategies for system-level design in hybrid electric vehicles. *IEEE T Veh Technol* 2016;66(1):57–70.
- [8] Sulaiman N, Hannan MA, Mohamed A, Ker PJ, Majlan EH, Daud WW. Optimization

- of energy management system for fuel-cell hybrid electric vehicles: Issues and recommendations. *Appl Energy* 2018;228:2061–79.
- [9] Malikopoulos AA. Supervisory power management control algorithms for hybrid electric vehicles: a survey. *IEEE T Intell Transp* 2014;15(5):1869–85.
- [10] Trovao JP, Pereirinha PG, Jorge HM, Antunes CH. A multi-level energy management system for multi-source electric vehicles - An integrated rule-based meta-heuristic approach. *Appl Energy* 2013;105:304–18.
- [11] Moura SJ, Callaway DS, Fathy HK, Stein JL. Tradeoffs between battery energy capacity and stochastic optimal power management in plug-in hybrid electric vehicles. *J Power Sources* 2010;195(9):2979–88.
- [12] Chen Z, Xiong R, Wang C, Cao J. An on-line predictive energy management strategy for plug-in hybrid electric vehicles to counter the uncertain prediction of the driving cycle. *Appl Energy* 2017;185:1663–72.
- [13] He H, Guo X. Multi-objective optimization research on the start condition for a parallel hybrid electric vehicle. *Appl Energy* 2018;227:294–303.
- [14] Lin CC, Peng H, Grizzle JW, Kang JM. Power management strategy for a parallel hybrid electric truck. *IEEE T Contr Syst T* 2003;11(6):839–49.
- [15] Yang Y, Pei H, Hu X, Liu Y, Hou C, Cao D. Fuel economy optimization of power split hybrid vehicles: A rapid dynamic programming approach. *Energy* 2019;166:929–38.
- [16] Peng J, He H, Xiong R. Rule based energy management strategy for a series-parallel plug-in hybrid electric bus optimized by dynamic programming. *Appl Energy* 2016;185:1633–43.
- [17] Sciarretta A, Back M, Guzzella L. Optimal control of parallel hybrid electric vehicles. *IEEE T Contr Syst T* 2004;12(3):352–63.
- [18] Sun C, Sun F, He H. Investigating adaptive-ECMS with velocity forecast ability for hybrid electric vehicles. *Appl Energy* 2017;185:1644–53.
- [19] Hu X, Murgovski N, Johannesson L, Bo E. Energy efficiency analysis of a series plug-in hybrid electric bus with different energy management strategies and battery sizes. *Appl Energy* 2013;111(4):1001–9.
- [20] Xie S, Hu X, Xin Z, Brighton J. Pontryagin's minimum principle based model predictive control of energy management for a plug-in hybrid electric bus. *Appl Energy* 2019;236:893–905.
- [21] Borhan H, Vahidi A, Phillips AM, Kuang ML, Kolmanovsky IV, Phillips A, Cairano SD. MPC-based energy management of a power-split hybrid electric vehicle. *IEEE T Contr Syst T* 2012;20(3):593–603.
- [22] Li L, You SX, Yang C, Yan B, Song J, Chen Z. Driving-behavior-aware stochastic model predictive control for plug-in hybrid electric buses. *Appl Energy* 2016;162:868–79.
- [23] Li L, You SX, Yang C. Multi-objective stochastic MPC-based system control architecture for plug-in hybrid electric buses. *IEEE T Ind Electron* 2016;99(1):1–12.
- [24] Hou C, Ouyang M, Xu L, Wang H. Approximate Pontryagin's minimum principle applied to the energy management of plug-in hybrid electric vehicles. *Appl Energy* 2014;115:174–89.
- [25] Onori S, Tribioli L. Adaptive Pontryagin's minimum principle supervisory controller design for the plug-in hybrid GM chevrolet volt. *Appl Energy* 2015;147:224–34.
- [26] Xie S, He H, Peng J. An energy management strategy based on stochastic model predictive control for plug-in hybrid electric buses. *Appl Energy* 2017;196:279–88.
- [27] Wang H, Huang Y, Khajepour A, Song Q. Model predictive control-based energy management strategy for a series hybrid electric tracked vehicle. *Appl Energy* 2016;182:105–14.
- [28] Tian H, Li SE, Wang X, Huang Y, Tian G. Data driven hierarchical control for online energy management of plug-in hybrid electric city bus. *Energy* 2018;142:55–67.
- [29] Liu T, Hu X, Li SE, Cao D. Reinforcement learning optimized look-ahead energy management of a parallel hybrid electric vehicle. *IEEE/ASME Trans Mechatron* 2017;22(4):1497–507.
- [30] Wu J, He H, Peng J, Li Y, Li Z. Continuous reinforcement learning of energy management with deep Q network for a power split hybrid electric bus. *Appl Energy* 2018;222:799–811.
- [31] Xiong R, Cao J, Yu Q. Reinforcement learning-based real-time power management for hybrid energy storage system in the plug-in hybrid electric vehicle. *Appl Energy* 2018;211:538–48.
- [32] Xu S, Li SE, Peng H, Cheng B, Zhang X, Pan Z. Fuel-saving cruising strategies for parallel HEVs. *IEEE Trans Veh Technol* 2016;65(6):4676–86.
- [33] Zhang X, Li CT, Kum D, Peng H. Prius (+) and volt(-): Configuration analysis of power-split hybrid vehicles with a single planetary gear. *IEEE T Veh Technol* 2012;61(8):3544–52.
- [34] Zhuang W, Zhang XW, Peng H, Wang LM. Simultaneous optimization of topology and component sizes for double planetary gear hybrid powertrains. *Energies* 2016;9(6):411.
- [35] Zhang X, Peng H, Sun J, Li SE. Automated modeling and mode screening for exhaustive search of double-planetary-gear power split hybrid powertrains. The ASME conference on automatic control, San Antonio, Texas; 2014.
- [36] Zhang X, Li SE, Peng H, Sun J. Design of multimode power split hybrid vehicles—a case study on the voltec powertrain system. *IEEE Trans Veh Technol* 2016;65(6):4790–801.
- [37] Zhuang W, Zhang X, Ding Y, Wang L, Hu X. Comparison of multi-mode hybrid powertrains with multiple planetary gears. *Appl Energy* 2016;178:624–32.
- [38] Zhang X, Li SE, Peng H, Sun J. Design of multimode power-split hybrid vehicles—a case study on the voltec powertrain system. *IEEE T Veh Technol* 2016;65(6):4790–801.
- [39] Chau KT, Chan CC. Emerging energy-efficient technologies for hybrid electric vehicles. *P IEEE* 2007;95(4):821–35.
- [40] Albers J, Meissner E, Shirazi S. Lead-acid batteries in micro-hybrid vehicles. *J Power Sources* 2011;196(8):3993–4002.
- [41] Stienecker AW, Stuart T, Ashtiani C. An ultracapacitor circuit for reducing sulfation in lead acid batteries for mild hybrid electric vehicles. *J Power Sources* 2006;156(2):755–62.
- [42] Lee BH, Shin DH, Kim BW, Kim HJ, Lee BK, Won CY, et al. A study on hybrid energy storage system for 42V automotive power-net. In: 2006 IEEE power and propulsion conference, Windsor, Canada, Sep 6-8; 2006. p. 1–5. doi: 10.1109/VPPC.2006.364310.
- [43] Liu Z, Ivanco A, Filipi ZS. Impacts of real-world driving and driver aggressiveness on fuel consumption of 48V mild hybrid vehicle. *SAE Int J Alternative Powertrains* 2016;5(2):249–58.
- [44] Martinez CM, Hu X, Cao D, Velenis E, Gao B. Energy management in plug-in hybrid electric vehicles: recent progress and a connected vehicles perspective. *IEEE T Veh Technol* 2017;66(6):4534–49.
- [45] Zhou X, Qin D, Hu J. Multi-objective optimization design and performance evaluation for plug-in hybrid electric vehicle powertrains. *Appl Energy* 2017;208:1608–25.
- [46] Hofman T, Ebbesen S, Guzzella L. Topology optimization for hybrid electric vehicles with automated transmissions. *IEEE T Veh Technol* 2012;61(6):2442–51.
- [47] Yang Y, Hu X, Pei H, Peng Z. Comparison of power-split and parallel hybrid powertrain architectures with a single electric machine: Dynamic programming approach. *Appl Energy* 2016;168:683–90.
- [48] Canova M, Guezennec Y, Yurkovich S. On the control of engine start/stop dynamics in a hybrid electric vehicle. *J Dyn Syst Meas Contr* 2009;131(6):636–50.
- [49] Liu C, Chau KT, Jiang JZ. A permanent-magnet hybrid brushless integrated starter-generator for hybrid electric vehicles. *IEEE T Ind Electron* 2010;57(12):4055–64.
- [50] Wang C, Yin C, Zhang T, Zhu T. Powertrain design and experiment research of a parallel hybrid electric vehicle. *Int J Auto Tech-kor* 2009;10(5):589–96.
- [51] Greencarcongress. Volkswagen launches new Passat GTE plug-in hybrid in Europe. <http://www.greencarcongress.com/2015/07/20150714-pasatgte.html>; 2015. [accessed 19.04.29].
- [52] Greencarcongress. Hyundai launches all-new Sonata Hybrid with GDI engine; plug-in hybrid variant coming next year. <http://www.greencarcongress.com/2014/12/20141217-sonata.html>; 2014. [accessed 19.04.29].
- [53] Greencarcongress. BYD's Qin plug-in hybrid the best selling automotive EV in China; 2014. <http://www.greencarcongress.com/2014/03/20140321-qin.html>; [accessed 19.04.29].
- [54] Greencarcongress. BYD Tang SUV PHEV available for pre-orders starting at \$48.3K before incentives. <http://www.greencarcongress.com/2015/01/20150123-tang.html>; 2015. [accessed 19.04.29].
- [55] Rahman Z, Ehsani M, Butler K. An investigation of electric motor drive characteristics for EV and HEV propulsion systems. *SAE Technical Paper No.2000-01-3062*; 2000.
- [56] Katrasnik T. Analytical framework for analyzing the energy conversion efficiency of different hybrid electric vehicle topologies. *Energy Convers Manage* 2009;50(8):1924–38.
- [57] Sundström O, Guzzella L, Soltic P. Optimal hybridization in two parallel hybrid electric vehicles using dynamic programming. *IFAC Proc Volumes* 2008;41(2):4642–7.
- [58] Rezaei A, Burl JB, Solouk A, Zhou B, Rezaei M, Shahbakhti M. Catch energy saving opportunity (CESO), an instantaneous optimal energy management strategy for series hybrid electric vehicles. *Appl Energy* 2017;208:655–65.
- [59] Chambon P, Curran S, Huff S, Love L, Post B, Wagner R, et al. Development of a range-extended electric vehicle powertrain for an integrated energy systems research printed utility vehicle. *Appl Energy* 2017;191:99–110.
- [60] Vijayenthiran V. BMW i3 Live Photos: 2013 Frankfurt auto show; 2014. http://www.motorauthority.com/news/1047387_2014-bmw-i3-live-photos-2013-frankfurt-auto-show; 2013. [accessed 19.04.29].
- [61] Greencarcongress. Report: Nissan to unveil new e-Power Juke concept at Tokyo show; 2nd application of new series-hybrid powertrain. <http://www.greencarcongress.com/2017/01/20170130-nissan.html>; 2017. [accessed 19.04.29].
- [62] Liu JM, Peng HE. Modeling and control of a power-split hybrid vehicle. *IEEE T Contr Syst T* 2008;16(6):1242–51.
- [63] Pei H, Hu X, Yang Y, Tang X, Hou C, Cao D. Configuration optimization for improving fuel efficiency of power split hybrid powertrains with a single planetary gear. *Appl Energy* 2018;214:103–16.
- [64] Miller JM. Hybrid electric vehicle propulsion system architectures of the e-CVT type. *IEEE T Power Electr* 2006;21(3):756–67.
- [65] Zhang X, Peng H, Sun J. A near-optimal power management strategy for rapid component sizing of multimode power split hybrid vehicles. *IEEE T Contr Syst T* 2015;23(2):609–18.
- [66] Hashimoto T, Yamaguchi K, Matsubara T, Yaguchi H, Takaoka T, Jinno K. Development of new hybrid system for compact class vehicles. *SAE Technical Paper 2009-01-1332*; 2009. doi:10.4271/2009-01-1332.
- [67] Vasilash GS. A lexus like no other but like the rest: introducing the RX 400h - luxury, not economy. *Automotive Design & Production* 2005;2:38–41.
- [68] Duhon AN, Sevel KS, Tarnowsky SA, Savagian PJ. Chevrolet volt electric utilization. *SAE Int J Alternative Powertrains* 2015;4(2):269–76.
- [69] Holmes AG, Schmidt MR. Hybrid electric powertrain including a two-mode electrically variable transmission. *United States patent US 6,478,705*; 2001 Jul 19.
- [70] Ngo HT, Yan HS. Novel configurations for hybrid transmissions using a simple planetary gear train. *J Mech and Robot* 2016;8(2):021020–21110. <https://doi.org/10.1115/1.4031952>.
- [71] Liu JM, Peng HE. A systematic design approach for two planetary gear split hybrid vehicles. *Vehicle Syst Dyn* 2010;48(11):1395–412.

- [72] Bayrak AE, Kang N, Papalambros PY. Decomposition-based design optimization of hybrid electric powertrain architectures: simultaneous configuration and sizing. *Design. J Mech Design* 2015;138(7).
- [73] Kang M, Kim H, Kum D. Systematic configuration selection methodology of power-split hybrid electric vehicles with a single planetary gear. In: ASME 2014 dynamic systems and control conference. 2014. American Society of Mechanical Engineers. San Antonio, USA, October 22–24; 2014. p. V001T15A001.
- [74] Kim H, Kum D. Comprehensive design methodology of input- and output-split hybrid electric vehicles. In search of optimal configuration. *IEEE-ASME T Mech* 2016;21(6):2912–23.
- [75] Zhang H, Zhang Y, Yin C. Hardware-in-the-loop simulation of robust mode transition control for a series-parallel hybrid electric vehicle. *IEEE T Veh Technol* 2016;65(3):1059–69.
- [76] Finesso R, Spessa E, Venditti M. Cost-optimized design of a dual-mode diesel parallel hybrid electric vehicle for several driving missions and market scenarios. *Appl Energy* 2016;177:366–83.
- [77] Rahman K, Anwar M, Schulz S, Kaiser E, Turnbull P, Schulz S, et al. The Voltec 4ET50 electric drive system. *SAE Int J Eng* 2011;4(1):323–37.
- [78] Adachi M, Endo H, Mikami T, Yagi K, Wakuta S, Uchida T. Development of a new hybrid transmission for RWD Car. SAE Technical Paper 2006-01-1339, 2006, doi:10.4271/2006-01-1339.
- [79] Kamichi K, Okasaka K, Tomatsuri M, Matsubara T, Kaya Y, Asada H. Hybrid system development for a high-performance rear drive vehicle. SAE Technical Paper 2006-01-1338, 2006, doi:10.4271/2006-01-1338.
- [80] Kato S, Ando I, Ohshima K, Matsubara T, Hiasa Y, Ohshima K, et al. Development of multi stage hybrid system for new lexus coupe. *SAE Int J Alternative Powertrains* 2017;6(1):136–44.
- [81] Okuda K, Yasuda Y, Adachi M, Tabata A, Suzuki H, Adachi M, et al. Development of multi stage hybrid transmission. *SAE Int J Alternative Powertrains* 2017;6(1):77–83.
- [82] Zhu FT, Chen L, Yin CL. Design and analysis of a novel multimode transmission for a HEV using a single electric machine. *IEEE T Veh Technol* 2013;62(3):1097–110.
- [83] Zhuang W, Zhang X, Zhao D, Peng H, Wang L. Optimal design of three-planetary-gear power-split hybrid powertrains. *Int J Auto Tech* 2016;17(2):299–309.
- [84] Hong S, Choi W, Ahn S, Kim Y, Kim H. Mode shift control for a dual-mode power-split-type hybrid electric vehicle. *P I MechG D-J Aut* 2014;228(10):1217–31.
- [85] Tomura S, Ito Y, Kamichi K, Yamanaka A. Development of vibration reduction motor control for series-parallel hybrid system. SAE Technical Paper 2006; No. 2006-01-1125.
- [86] Yang C, Song J, Li L, Li S, Cao D. Economical launching and accelerating control strategy for a single-shaft parallel hybrid electric bus. *Mech Syst Sig Process* 2016;76:649–64.
- [87] Hwang HY. Minimizing seat track vibration that is caused by the automatic start/stop of an engine in a power-split hybrid electric vehicle. *J Vib Acoust* 2013;35(6):061007.
- [88] Kum D, Peng H, Bucknor NK. Control of engine-starts for optimal drivability of parallel hybrid electric vehicles. *ASME J Dyn Syst Meas Contr* 2013;135(2):450–72.
- [89] Chen L, Xi G, Sun J. Torque coordination control during mode transition for a series-parallel hybrid electric vehicle. *IEEE T Veh. Technol.* 2012;61(7):2936–49.
- [90] Zhuang W, Zhang X, Li D, Wang L, Yin G. Mode shift map design and integrated energy management control of a multi-mode hybrid electric vehicle. *Appl Energy* 2017;204:476–88.
- [91] Syed FU, Kuang ML, Ying H. Active damping wheel-torque control system to reduce driveline oscillations in a power-split hybrid electric vehicle. *IEEE T Veh Technol* 2009;58(9):4769–85.
- [92] Chen JS, Hwang HY. Engine automatic start-stop dynamic analysis and vibration reduction for a two-mode hybrid vehicle. *P I MechG D-J Aut* 2013;227(9):1303–12.
- [93] The official U.S. government source for fuel economy information. <https://www.fueleconomy.gov/>. [accessed 19.03.01].
- [94] Silvas E, Hofman T, Serebrenik A, Steinbuch M. Functional and cost-based automatic generator for hybrid vehicles topologies. *IEEE/ASME T Mechatronics* 2015;20(4):1561–72.
- [95] Ing AH. Automated topology synthesis and optimization of hybrid electric vehicle powertrains 2014. Thesis. University of Waterloo.
- [96] Bayrak AE, Ren Y, Papalambros PY. Topology generation for hybrid electric vehicle architecture design. *J Mech Design* 2016;138(8).
- [97] Filippa M, Mi C, Shen J, Stevenson RC. Modeling of a hybrid electric vehicle powertrain test cell using bond graphs. *IEEE T Vehicular Technology* 2005;54(3):837–45.
- [98] Zhang X, Li SE, Peng H, Sun J. Efficient exhaustive search of power-split hybrid powertrains with multiple planetary gears and clutches. *ASME J Dyn Syst Meas Contr*; 137(12): 121006.
- [99] Tarjan R. Depth-first search and linear graph algorithms. *SIAM J Comput* 1972;1(2):146–60.
- [100] Zhuang W, Zhang X, Peng H, Wang L. Rapid configuration design of multiple-planetary-gear power-split hybrid powertrain via mode combination. *IEEE-ASME T Mecha* 2016;21(6):2924–34.
- [101] Yoshimura T. Vehicle power transmission device. United States patent US Patent 8,535,189. Jun 17 2017.
- [102] Pan Z, Zhang X, Silvas E, Peng H, Ravi N. Optimal design of all-wheel-drive hybrid pick-up trucks. In: ASME 2015 dynamic systems and control conference. Columbus, USA, October 28–30; 2015. p. V001T10A002.
- [103] Qin Z, Luo Y, Zhuang W, Pan Z, Li K, Peng H. Simultaneous optimization of topology, control and size for multi-mode hybrid tracked vehicles. *Appl Energy* 2018;212:1627–41.
- [104] Zhuang W, Zhang X, Yin G, Peng H, Wang L. Mode shift schedule and control strategy design of multimode hybrid powertrain. *IEEE T Control Syst Technol* 2019. Feb 11.
- [105] Zhang S, Xiong R, Zhang C. Pontryagin's minimum principle-based power management of a dual-motor-driven electric bus. *Appl Energy* 2015;9:370–80.
- [106] Wu X, Hu X, Yin X, Li L, Zeng Z, Pickert V. Convex programming energy management and components sizing of a plug-in fuel cell urban logistics vehicle. *J Power Sources* 2019;423:358–66.
- [107] García A, Monsalve-Serrano J, Sari R, Dimitrakopoulos N, Tunér M, Tunestål P. Performance and emissions of a series hybrid vehicle powered by a gasoline partially premixed combustion engine. *Appl Therm Eng* 2019;150:564–75.
- [108] Xu S, Li SE, Cheng B, Li K. Instantaneous feedback control for a fuel-prioritized vehicle cruising system on highways with a varying slope. *IEEE T Intell Transp* 2016;18(5):10–1220.
- [109] Lin Q, Li SE, Du X, Zhang X, Peng H, Luo Y, et al. Minimize the fuel consumption of connected vehicles between Two Red-signalized intersections in urban traffic. *IEEE T Veh Technol* 2018;10:9060–72.
- [110] Vahidi A, Sciarretta A. Energy saving potentials of connected and automated vehicles. *Transportation Res Part C: Emerging Technol* 2018;95:822–43.
- [111] Hu J, Shao Y, Sun Z, Bared J. Integrated vehicle and powertrain optimization for passenger vehicles with vehicle-infrastructure communication. *Transportation Res Part C: Emerging Technol* 2017;79:85–102.
- [112] Sulaiman N, Hannan MA, Mohamed A, Majlan EH, Daud W. A review on energy management system for fuel cell hybrid electric vehicle: issues and challenges. *Renew Sustain Energy Rev* 2015;52:802–14.
- [113] Bendjedja B, Rizoug N, Boukhnef M, Bouchafaa F, Benbouzid M. Influence of secondary source technologies and energy management strategies on energy storage system sizing for fuel cell electric vehicles. *Int J Hydrogen Energy* 2017;43(25). S0360319917311722.
- [114] Das H, Tan C, Yatim A. Fuel cell hybrid electric vehicles: A review on power conditioning units and topologies. *Renew Sustain Energy Rev* 2017;76:268–91.
- [115] Hu X, Murgovski N, Johannesson LM, Egardt B. Optimal dimensioning and power management of a fuel cell/battery hybrid bus via convex programming. *IEEE/ASME Trans Mechatron* 2014;20(1):457–68.
- [116] Sorrentino M, Cirillo V, Nappi L. Development of flexible procedures for co-optimizing design and control of fuel cell hybrid vehicles. *Energy Convers Manage* 2019;185:537–51.
- [117] Zhang H, Li X, Liu X, Yan J. Enhancing fuel cell durability for fuel cell plug-in hybrid electric vehicles through strategic power management. *Appl Energy*. 2019;241:483–90.
- [118] Veneri, Ottorino. Technologies and applications for smart charging of electric and plug-in hybrid vehicles. Springer; 2017.
- [119] Kaltschmitt M, Themelis NJ, Bronicki LY, Söder L, Vega LA. Renewable Energy Systems. Springer; 2013.
- [120] Rubino L, Capasso C, Ottorino V. Review on plug-in electric vehicle charging architectures integrated with distributed energy sources for sustainable mobility. *Appl Energy* 2017;207:438–64.
- [121] Hui H, Ding Y, Shi Q, Li F, Song Y, Yan J. 5G network-based Internet of Things for demand response in smart grid: A survey on application potential. *Appl Energy* 2020;257. 113972.